Response to R1#

General comments

In this paper, the authors did a nice job to design a high quality air-sea flux tower (YXASFT) in Yongxing Islands for air-sea boundary layer flux-related observations. The instrumentation and the real-time data acquisition system were well designed. Then the authours evaluated the widely used WHOI OAflux reanalysis datasets using in suit data observed from YXASFT. Seasonal comparisons were quantitative analyzed between the OAflux and YXASFT observations by calculating the coefficient of determination, root-mean-square errors, and biases. Through seasonal comparison, the authors get innovative conclusions that the relaibility of OAFlux reanalysis datasets is associated with the monsoon system in SCS, which mainly manifested in the following aspects: 1. OAFlux provides a better estimation of *U* (Q_a) in the spring and winter characterized by a stronger (drier) northeast monsoon than in the summer_autumn characterized by a relatively weaker (wetter) southwest monsoon 2. The OAFlux *LHF* performance is better during the spring and winter than in the summer_autumn, which is further associated with the monsoon climate in the SCS.

The authors also quantified the biases in *SHF* and *LHF* of the OAFlux datasets and investigated the reasons that may be responsible for the biases. They found that the bias in Q_a is the main source of error for the LHF in winter monsoon period. Meanwhile, both biased in Q_a and U are responsible for controlling the biases in *LHF* during summer monsoon period. Biases in T_s are responsible for controlling the biases in SHF, and the effects of biases in T_s on the biases in *SHF* during the spring and winter are much greater than that in the summer_autumn period. At last, the authors suggest that both T_s and *SHF* in OAflux are the most unreliable data which should be used with considerable cautions to drive ocean models. Additionally, U, Q_a and *LHF* should be used with proper consideration due to their seasonal reliability variations. Researchers should feel more at ease using these data during the winter monsoon than in the southwest monsoon.

In general, the paper is well-written. Given the importance of the OAflux reanalysis products in the air-sea interaction community, it is worthwhile to systematically evaluate the accuracy of each variable. South China Sea is a region that is lack of sufficient air-sea interaction observations. The authors carried out in suit observations from air-sea tower in this region within relatively long periods, which is of great significance to improve the reliability of reanalysis datasets. The presentation of the results and conclusions are clear. Thus I recommend the paper to be accepted and published in AMT with minor to moderate revisions. I give the following suggestions to help the authors further improve the paper.

Response: Thanks for your time, We are pleased to note the favorable comments of anonymous reviewer in his (her) review of our manuscript entitled “Evaluation of OAFlux datasets based on in situ air-sea flux tower observations over the Yongxing Islands in 2016”. We have studied theire comments and suggestions carefully and

have made corresponding corrections which we hope meet with his (her) approval. All the corrections are underlined in red and the revised manuscripts was also enclosed as .pdf supplement in AMTD open forum.

Response to specific comments

1. As mentioned in the first question of the Specific comments, the reviewer suggest us to add more detailed observation system description mounted on YXASFT.

   Response: The hardware and online data acquisition programme of the observation system was jointly designed by the first author and the CSI (Campbell Scientific, Inc) engineers. We think this part is not very much related to the core study content of the paper, so we just use a brief sentence introduces the system architecture and fig.2 are enclosed for your information. We also applied for the Chinese invention patent of this air-sea boundary layer observation system, if the readers want to know more about this YXASFT and its observation system, can send E-mail to the corresponding author, we will send hardware and data acquasition programme for your reference.

2. What's the meaning of SEx, VXx, Px, Ixx…, it's a signal, or protocol standard, or sensor hardware interface?

   Response: Abbreviations such as SEx, VXx, Px, Ixx appears in Fig.2 are different signal output or input channels in CR3000 datalogger. Take channel SEx for example, it's the channel Signle-Ended Analogy input (CR3000 has 16 channel of SE). I added a reference of CR3000 USER'S MANUAL in Figure 2's caption.

3. In addition, I pay more attention to the data sharing and data quality. Whether the data can be open access directly by contract the communication author after the publication of the paper? What is the data format? Wheather the necessary data quality control is taken?

   Response: Of course, after the publication of the paper, the field observation data used in the YXASFT can be obtained from the authors via email to the corresponding author, we welcome more researchers using the data to verify the conclusions in this paper or carry out more in-depth research study. The data was prvided in the form of .dat, .xls and .txt with a data description header such as:
   Time stamp (YY/MM/DD HH:MM:SS), Wind speed (m/s), Wind direction (°),
   Air temperature (℃) and so on. Yes, we indeed do the necessary data quality control by despiking and averaging. The first hand observation data was obtained directly from data tables stored in CR3000 CF card, CR3000 scan sensors in a 1Hz frequency, an average value (the average value of the 1800 sets of data) was stored in data tables in every 30 mins, despiking was performed before averaging. For each variable, a spike is defined as a value that exceeding window mean ± 3.5 standard deviations over a certain time window (set to 5 min). Detected spikes

were identified and replaced based on a linear interpolation of neighboring values.

4. I visited the data sharing website listed in Page 3, line 17 and found that the web is in Chinese, it's not convinent for non Chinese readers, also I could not found the data download link.

   Response: Thanks for your suggestions and visiting our data website. Yes, the first version of this data sharing website was developed in Chinese language. After all the functions of the website passed running test, we will upgrade this website to both Chinese and English editions. The Login: CSL-CER and password: ruhuna metioned in the paper is only for real-time data and historical data curve display, to download the data files readers should contract the corresponding author for a new authorized username and password and a data sharing agreement must be signed, you can re-login the system with this new username and password, then data download link works.

5. In sec 3.1, the authors did a nice job to validate COARE3.0 using the direct eddy convariance flux (ECF) measurements, the verifying results are convincing. However, they didn't give descriptions of the EC data processing steps and the algorithm taken by each step. As I know that the EC method is mathematically complex, and significant care is required to set up different processing steps for different sites, measurements and study purposes, the difference in the processing algorithm can result in the difference between the turbulent fluxes results. I suggest the authors to add a brief description on how the fluxes are parameterized and calculated for the ECF trubulent data. The authors can also add a figure to express the ECF data processing flow more clearly. For instance, which algorithms were adopted for coordinatate rotation and WPL compensation?

   Response: Thanks for your suggestion, in this paper the directly measured eddy convariance heat fluxes by IRGASON ECF system was used to verify the performance of COARE3.0. The online flux calculation program EasyFlux_DL developed by CSI was run in CR3000, the turbulent data processing steps are as follw: despiking [Vickers et al., 1997], Coordinate rotation [van Dijk et al., 2004], frequency correction [Moncrieff et al., 2004], WPL compensation [Wallace et al., 2006].As suggested by reviewer, I added **figure 3** to show the data processing flow of EC data in the paper.

6. According to the description of in suit data in the paper, I realized that the wind speed range in the YXASFT observed data covers typhoon force winds, as there were at least 2 strong typhoons (No.1603 "MARINAE" and No.1624 "SARIKA") passed through Xisha sea area. So I suggest the authors to add discussions on how COARE3.0 algorithm performs compared to observed exchange coefficients for high wind conditions.

Response:

Parameterization of exchange coefficients in high wind is a hot topic in recently years. Both laboratory results [Haus et al., 2010] and field observations [Zhang et al., 2008] indicated that the variations of exchange coefficients in high wind were quite different from that in moderate wind. Some of our observed wind speed reached the high wind level, however, for parametric studies, high frequency observations from several Hz to tens of Hz are essential based on the eddy covariance (EC) method. In this study, the EC system installed on YXASFT only worked for two months from 1st Feb to 29th Mar, and no typhoon passed through Xisha during this period. Consequently, the exchange coefficients could not be obtained from in situ data and the observational LHF was calculated by the bulk method COARE 3.0. Our limited knowledge of the parameterization of exchange coefficients would probably, to some degree, lead to uncertainties in the estimates of LHF under high wind conditions. This is a problem remains to be ameliorated with more available observational data under extreme conditions in the future. It is also an important way to develop more reliable and applicable parameterization schemes for exchange coefficients to improve performances of the LHF products.

Response to technical corrections:

We found the referee's comments on this part are most helpful, we accepted the corrections and suggestion listed from 1st to 21th in the technical corrections, and make corrections in the corresponding place with underlined in red. With regard to the 22th and 23th suggestion, we adjusted the colour of all the figures and deleted the relevant passage since they are not essential to the contents of the paper.

Response to R2#

General comments

The main aim of this study is to assess the comparisons of latent (LHF) and sensible (SHF) heat fluxes from the high quality Yongxing air-sea flux tower (YXASFT) and OAFlux data. YXASFT LHF and SHF are calculated from bulk variables derived from instrument measurements, while OAFlux fluxes are available as global daily re-analyses with a spatial resolution of 1 ° in longitude and latitude. The authors handled interesting and needed work aiming at the estimation of heat fluxes. However, the paper requires scientific improvements. I would suggest to further clarify the study objective and the main new findings. The main results, shown in this paper, deal with straightforward comparisons of YXASFT and OAFlux daily flux estimates, with few insights in the physics and the spatial and temporal scale impacts on the comparison results. The paper does not investigate the quality of YXASFT heat fluxes. The results showing the comparison between YXASFT and ECF fluxes are not convincing. The comparisons between the two sources are quite poor. OAFlux flux estimates have been investigated in several papers, including in papers published by the

authors. For instance, the bias characterizing mean difference between moorings and OAFlux LHF are quite small. In this study, the LHF biases exhibit "outstanding" values. It would of great interest for scientific community to understand the source of differences between the previous published results and those shown in this manuscript. I am feeling very sorry. I cannot recommend the publication of this paper. However, I strongly encourage the authors to consider the comments aforementioned and listed hereafter for a new enhanced version.

Response: Thank you very much for your review and objective comments on this study. First of all, we should acknowledge that this study focuses more on the in situ measurement techniques and less on the relevant physical processes or other scientific questions. Actually, for a long time in the past, we have been devoted to the construction of YXASFT by installing variety of observational sensors and uninterrupted maintenance work, with the aim of making it a unique, fixed, multi-parametric and long-term observational tower of air-sea interaction that is still running normally in the open water of the SCS. This study focuses on the introduction of the YXASFT and presenting some preliminary results. To prove the reliability of these in situ observations, we compared the two observational results of high frequency (ECF turbulent flux) and low frequency (bulk flux) at the beginning. In general, the results of LHF in the two sources are in good agreement. Note that some obvious mismatches can be found, which is mainly due to the effect of precipitation of ECF flux data. However, for SHF, variations in the two sources are quite different and big discrepancies exist in them. This partly due to the deficiency of the ECF sensors in the measurement of air temperature, and on the other hand it is related to the defect of the bulk formula in the SHF calculation. We have explained this with more detail under the response to Specific comments No.6. As one of the most representative flux products, the OAFlux datasets was chosen and compared with full year observations at YXASFT. The YXASFT observations and OAFlux estimates coincide relatively well. On the one hand, this enhanced our confidence on the reliability of YXASFT observations. On the other hand, it helps to find problems in the present flux product and find ways to improve them.

Generally speaking, we presented all the problems found in the comparisons and gave possible explanations for every mismatch, which can provide references for YXASFT and OAFlux data users. However, considering the fact that the nature of AMT is focused more on the observation technology, we have not made a deep analysis of the reasons for these problems and related scientific issue. In the future work, with the continuous accumulation of high quality YXASFT observation data, we will focus more on the scientific issues related to the air-sea boundary layer interaction.

As the technical director of the YXASFT for its design and maintenance, I have received many requests for data sharing of YXASFT in different private (E-mails, messages from CAS, NUSIT, OUC et al.,) and public occasions (EGU, AGU and AOGS exhibitions). And the publication of this article can greatly enhance our confidence and promote efforts to obtain the in situ observations which are very important to air-sea interaction scientific research around the SCS.

At last, we have studied the comments carefully, gave explanation for each questions list below and made some corresponding corrections which we hope meet with your approval.

Specific comments

1. Page 3, Line 23: The correction procedure used for the estimation of Tau, SHF, and LHF should be explained.

Response: Thanks for your suggestion, due to the limited article space, we did not give a detail description of EC data processing step in the paper. The turbulent flux was calculated by an online program named EasyFlux_DL, which was developed by Campbell Scientific Inc, each EC data processing steps we adopted in EasyFlux_DL are as follws: despiking (Vickers et al., 1997), Coordinate rotation (van Dijk et al., 2004), frequency correction (Moncrieff et al., 2004), WPL compensation (Wallace et al., 2006). As suggested by reviewer, we added **Figure 3** (Page 22 in the revised paper) to show the EC data correction procedure. And also, in Page 6, Line 11-14, we have added a description of the EC data processing, as follows:

"The EC method is mathematically complex, significant care is required to set up different processing steps for different sites, measurements and study purposes. In this paper, the EC program running on CR3000 was based on the processing steps shown in Fig. 3. "

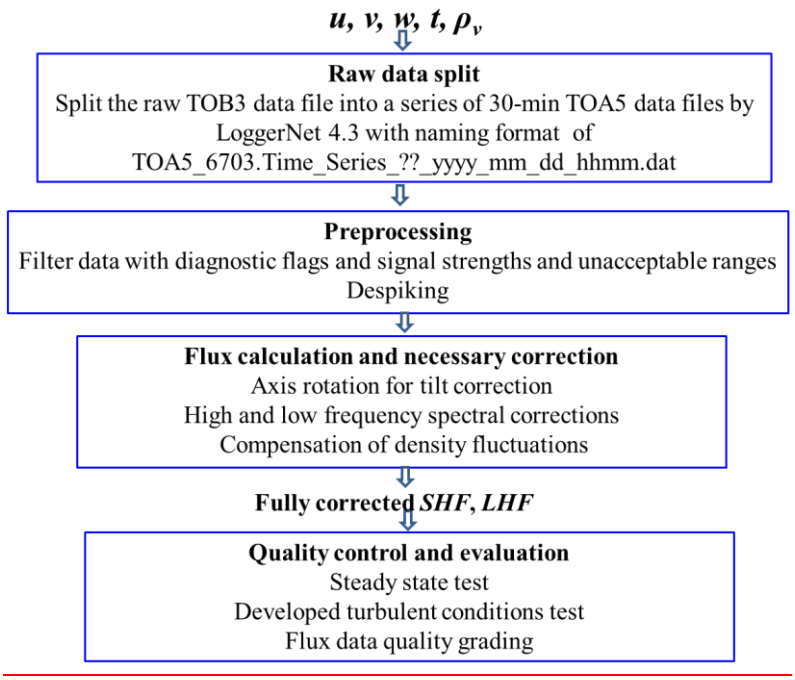

Fig.3 (in the revised paper). EC turbulence data processing and quality control flow chart

2: Page 4: Are bulk variables measured at 20m, 12m, or 10m? The manuscript shows all these values, but does not mention any height correction.

Response: The U in YXASFT used for comparison were measured in 10m, this is the same height with surface layer U in the OAFlux. The T_a and Q_a adopted in YXASFT were measured at 5m, while the measurement height of T_a and Q_a in the OAFlux are

both 2m. Thus, prior to conducting a comparison, we used the height correction algorithm for bulk variables provided in COARE3.0 to correct the YXASFT observed data to the same height as the bulk variables in OAFlux. This was already explained in the paper (marked by red color), in Page 4, Line 18-20, as follow:
"The measurement heights of T_a and Q_a in the OAFlux dataset are both 2m, while the measurement heights for these two parameters on the YXASFT are both 5m. Thus, prior to conducting a comparison, we corrected the corresponding heights of the in situ data to correspond to the variable heights in the OAFlux dataset using COARE3.0. "

3. Page 3, Line 13: OAFlux are not measurements. They are estimates.

Response: Thank you for reminding us. Yes, OAFLux is an estimated product with the synthesis of reanalysis and satellite inputs. The improper expression and all the similar problems found in the manuscript have been corrected.

4. Page 5, Lines 18 – 25: It is not clear. Are these calculates handled by the authors or by dedicated online software. The authors mention above the use of Easy-flux software.

Response: In recent years, many EC data processing methods has been developed and updated, which are mainly divided into two kinds: one is the post-processing software, such as EdiRe, EddyPro, TK3 and so on. The users can use these software to process the direct measured high frequency turbulent data, the built-in correction algorithm module can be selected with purpose to adapt the location and environment of the observation site. The other is online processing program, such as the Easy_flux developed by Campbell Scientific Inc, which requires the user to preset the adaptive correction algorithm in the program according to the site location and the surrounding environmental condition, the program can calculate the turbulent flux in 30min or 60min in real time. The built in algorithm modules of the online program and post-processing softwares are universally accepted around the world, the calculation results are also very similar.
In this paper, we directly use the flux calculation results of the Easy_flux online program to compare with bulk heat fluxes. Further, considering the special location of the island reef and the underlying surface of sea water, we preset a suitable data correction algorithm in order to assure the reliability of the observed data, such as we select planar fitting method for axis correction of sonic wind sensor. A detailed response has been made in Specific comments No.1 in regard to the correction procedure.

5. Page 6, Lines 19 – 24: Do the authors assume that ECF LHF observations are overestimated for rain events? Does it result from instrumental and/or measurement issues?

Response: Yes, due to the limitation of the measurement principle of EC sensors, precipitation has great influence on the measurement of high frequency of Q_a and T_a (T_a was indirect measured by the ultrasonic, however the principle of ultrasonic

measurement of T_a will be seriously affected by precipitation). So, this is a technical problem that has not yet been solved well around the world. Due to there is no direct precipitation observation in the YXASFT, we plot the time series of the 30 min mean variables of U, T_a and Rh in Fig.1 (but this figure was not added in the revised article). As we can see from Fig.1, the time window of four possible precipitations were in 2016/02/03, 2016/02/07, 2016/02/25, 2016/03/26 (marked by dashed ellipse), respectively, which could be obviously shown from a sudden increase in Rh and a sudden drop in T_a.

Strictly speaking, the ECF data in these four time windows must be eliminated before compared with COARE3.0. In this paper, we didn't eliminate the possible data polluted by precipitation, but it almost does not affect the validation of LHF. The LHF comparison between ECF and COARE3.0 shows a good consistency except for the above mentioned possible precipitation windows. We agree very much that if the ECF data during precipitation days were eliminated, the comparison between CAORE3.0 and ECF will be more consistent, which will further demonstrate the reliability of the COARE3.0 algorithm in SCS.

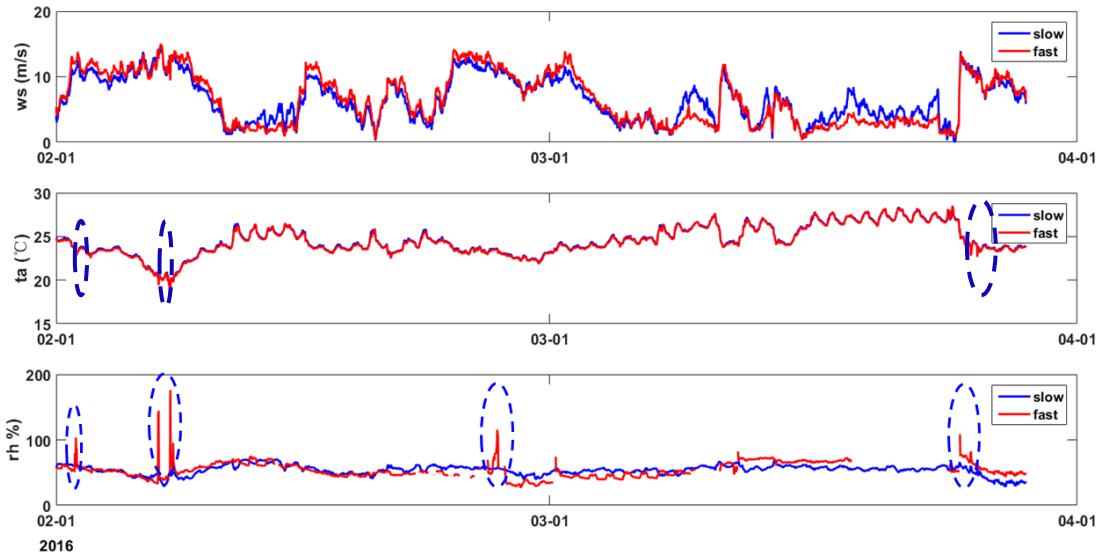

Fig.1 Time series of observed wind speed (U), air temperature (Ta), air relative humidity (Rh) by the slow and fast response sensors, respectively. The time windows for possible precipitation were marked by dashed ellipse.

6. Page 7, Lines 25 – 28: Convincing scientific and/or technical reasons should be provided for explaining the difference between observed and estimated SHF.

Response: The big difference of SHF between ECF and bulk method can be attributed to both the technical and theoretical reasons.

Technical aspects: As we mentioned in the answer of the last question, the T_a was indirectly measured using ultrasonic principle rather than directly physical measurement, so it was easily affected by the precipitation and surrounding environment **(Zhang et al., 2016)**. Further more, T_a was the key factor of SHF calculation and can directly affect the accuracy the SHF in ECF system. So,

inaccuracy measurement of T_a by ECF system is a technical problem to be solved.
Theoretical aspects: The present bulk method still has large uncertainties in SHF calculation (for example, the uncertainty and limitations of parameterization schemes), which can affect the calculation accuracy of SHF by bulk method. To solve this problem, joint efforts by the scientific community are needed to improve and optimize the parameterization scheme
So, on the basis of the technical and theoretical problems mentioned above, the comparison results show that the SHF calculated by ECF and Bulk method is so not consistent with each other. Actually, this problem is well understood as: you can not expect that neither of the two results is accurate enough to have good match with each other.
Further, from Fig.9 in the revised paper we can find that the SHF deviation of YXASFT observation and OAFlux is mainly come from spring and winter, but it showed high consistency in the summer_autumn period. This is also consistent with the T_s comparison in Fig.7, which are further affected by the cloud cover in different seasons.

Reference:

Zhang R., J. Huang, X. Wang, J. A. Zhang, and F. Huang, 2016: Effects of precipitation on sonic anemometer measurements of turbulent fluxes in the atmospheric surface layer. J. Ocean Univ. China, 15(3), 389-398.

7. Page 7, Lines 11-13: How the YXASFT and OAFlux consistency has been determined?

Response: One side, we try to understand your question from the aspect of spatial matching of the compared datasets. Reply as follows:
The YXASFT observation is a signal point, and the OAFlux is a gridded datasets. In order to minimize the uncertainly caused by the location difference, we have adopted the method introduced by **(Sun et al, 2003)**. The representative OAFlux data used for comparison with YXASFT is derived by bilinearly interpolated (inversely weighted by distance) from values of the surrounding four grid points.
On the other side, we try to understand your question as how to quantify of data consistency from the comparison, and reply as follows:
We gave both the time series and the scatter plots of each compared variables in Fig.5 and Fig.7 (in the revised paper), respectively. From Fig.7, the consistency of the two variables can be quantitative analyzed by value of both line coefficient and R^2, the bigger value of line coefficient and R^2 indicates a better consistency.

Reference:

Sun B, Yu L, Weller RA (2003). Comparisons of surface meteorology and turbulent heat fluxes over the Atlantic: NWP model analyses versus moored buoy observations. Journal of Climate 16:679–695.

8. Page 8, Lines 1-2: The OAFlux U biases are quite high compared to those obtained from moored buoys and OAFlux U10 comparisons. Does this result relies on

YXASFT location and/or on OAFlux spatial and temporal resolutions?

Response: Overall speaking, the U10 of OAFlux is in good consistent with the YXASFT observation, with bias of 0.96m/s in Spring, 1.19m/s in Summer_Autumn and 0.67m/s in Winter, and a R^2 of 0.90 in Spring, 0.79 in Summer_Autumn and 0.92 in Winter, respectively. However, as shown in Fig.5 and Fig.7 (first row), the U10 in OAFlux is slightly higher than YXASFT observation, and the U10 difference between OAFlux and YXASFT is more obvious in summer. The reason for this may be related to the onset of the summer monsoon and the environmental factors became more complex during this period. The problem of the larger U10 difference between OAFlux and YXASFT during the monsoon period remains to be further studied.

On the other hand, the mismatch in temporal and spatial resolution may also affect the high biases in U. OAFlux is grid data and YXASFT is a single point observation data, the two datasets for comparison can bot be fully spatial matched. So this spatial difference may also lead to the mismatch between of OAFlux and YXASFT observation. The observed daily average data were derived from the average of 48 high-frequency (30 min) observations, but the temporal resolution of the OAFlux's daily average data is not so high (6 hours satellite remote sensing data), so the temporal resolution difference may also lead to the mismatch in their daily average data.

9. Page 8, Lines 22-24: The cloud impact on OAFlux T_s (from NOAA OI SST) should be found everywhere, and especially along tropical are. The previous published studies aiming at the assessment of OAFlux daily data, did not provide T_s results shown in this study.

Response: Yes, this suggestion (the available OLR reanalysis data download) has also been given by a Short Comment during the public discussion period. And, we downloaded the daily mean OLR data from NOAA through this web link: https://www.esrl.noaa.gov/psd/cgi-bin/db_search/DBSearch.pl?Dataset=NOAA+Uninterpolated+OLR&Variable=Outgoing+Longwave+Radiation, also we plotted the OLR time series as Fig 2. But from OLR time series, we can not infer that the cloud cover of the sky in winter and spring is more than that during the summer monsoon period (2016/5-2016/9). Then we used DLR (downward longwave radiation) observed from YXASFT to estimate cloud cover indirectly instead of OLR. As we know, DLR is mainly depends on the air temperature, which can be affected by cloud cover. When the sky was covered with large clouds and thick clouds, the probability of rising air temperature will be bigger, which will further increase the DLR. We plotted the curve of observed DLR in Fig.8 (in the revised paper) in the revised paper, from Fig.8 we can see that there is an evidently greater fluctuation in the DLR during the winter and spring periods than in the summer_autumn period, indicating that the winter and spring seasons possess greater probabilities of cloudy days.

Yes, as shown in the previous study, with the onset of the summer monsoon, the sky cloud cover should increase, and the T_s retrieved via the AVHRR should correspondingly exhibit a lower quality. But in this study, we found a different result that the data quality of T_s in OAFlux during the monsoon period is better than that in

spring and winter season. And also we have tried to use the observed DLR to explain this phenomenon was caused by the less cloud cover during the summer monsoon period. This interesting phenomenon may be caused by the fact that the intensity of the summer monsoon in 2016 was weaker than those in preceding years, which remains further explored.

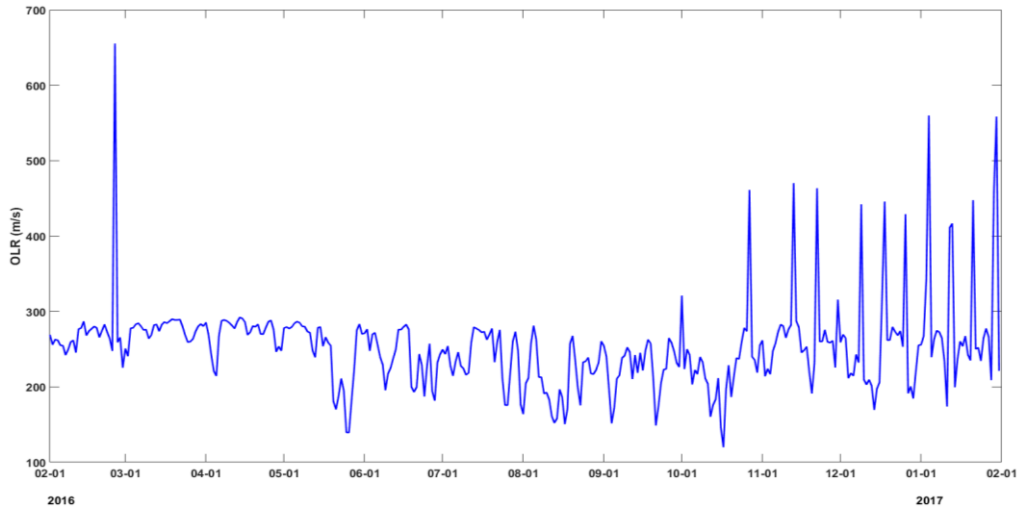

Fig 2. Daily mean of NOAA OLR from 2016//02/01-2017/01/31

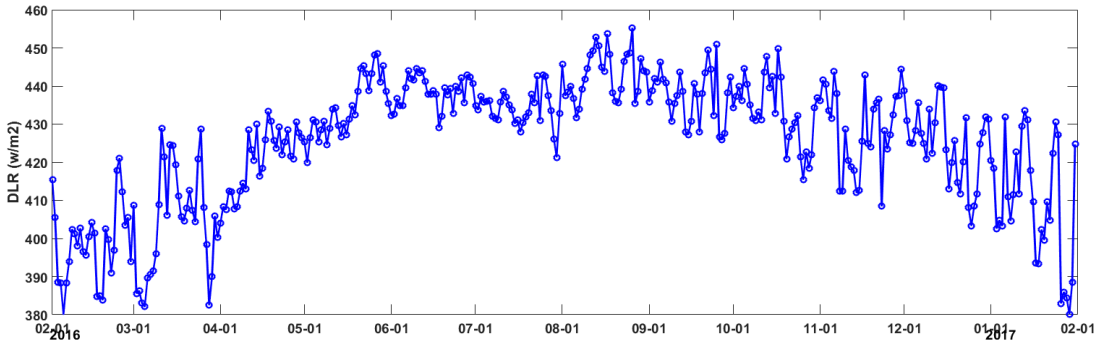

Fig 8 (in the revised paper). Daily mean time series plots of the YXASFT-observed downward long radiation (DLR) over the study period (2016/02/01-2017/01/31).

10. Page 10: The section on top only confirms the results published in several papers. It does provide any new findings dealing with the assessment of LHF and SHF quality or accuracy. Figure 9 and 10 show some interesting results. For instance, the relationship between ΔLHF and ΔTa for winter, would be investigated. Furthermore, the figures show significant scatter. The latter would be investigated as study cases.

Response: Yes, in terms of biased factor that determine the biased heat flux, we have got some conclusions similar to previous studies. Such as, the biases in T_s were the key factor dominating the biases in SHF and the biases in LHF is mainly caused by the biases in Q_a. This does not seem redundant in the article, but proves the credibility

of both previous and the present studies. And, we further analyzed the bias factors that dominate the biase of heat flux in different seasons. For example, from Fig.10 (in the revised paper), it can be seen that the LHF bias between YXASFT and OAFlux mainly caused by biased Q_a in Spring, biased U and Q_a in Summer_Autumn, and bised Q_a and T_a in winter, respectively. These dominate factors that cause the seasonal biases in heat flux are new findings in this article. Thank you for your suggestions, we have revised this chapter in Page 9&10, Line 26-33 & 1-3, as follows:

Δ LHF: The biases in Q_a are the most dominant factor in determining the biases in LHF during the spring with relatively high R^2 values of 0.38 compared with the other biased bulk variables (Fig. 10 (first column)). Both of the Q_a and U biases are responsible for controlling the biases in LHF during the summer_autumn period with R^2 values of 0.36 and 0.32, respectively (Fig. 10 (second column)). Both of the Q_a and T_a biases are the dominate factors in determining the bias in LHF during the winter period with R^2 values of 0.43 and 0.16, respectively (Fig. 9 (third column)). The biases in T_s is negligible control factors on the biases in LHF, since their R^2 values are all relatively small during the three periods compared with those of Q_a (Fig. 9 (third and fourth rows)). In general, the result revealed that the Q_a is the most dominated factor controlling the biases in LHF throughout the year is similar to those reported in previous studies (Wang et al., 2013, 2017). Additional, these dominate factors that cause the seasonal biases in LHF are new findings in this article.

Yes, it is true that we can find some special phenomena from scatter plots in Fig.10 and Fig.11 (in the revised paper). As you mentioned, from Fig.10, we can see that the relationship of biased LHF and biased T_a in winter is very different from that in spring and summer_autumn, this can be further investigated as a phenomenon study case. This is a good advice, but the main purpose of this paper is to compare the YXASFT observation data and the OAFlux reanalysis data, present the results of comparison objectively, prove the reliability of the observation data, provide references and suggestions for data users. Any in-depth analysis of phenomena or physical process is not described in this paper, but will be further explored in the follow-up research work.

Response to SC1#

Short Comments

The high-quality measurements from the YXASFT are extremely precious for the study of SCS-related air-sea exchange processes. The authors have carried out three works: 1) testing the reliability of the COARE3.0 bulk algorithm in the SCS, 2) comparing the seasonal variations between the WHOI OAFlux products and YXASFT observations, and 3) finding the possible sources of the biases in LHF and SHF. These works are very interesting and important for understanding the effectiveness of the presented algorithm (COARE3.0) and data (OAFlux) when using in the SCS, which is helpful for conducting the future SCS-related works. Looking forward to reading the final copy of this paper.

Response: Thank you for your praise of the article and the recognition of the author's research work. Exactly, what we done in the paper is to effectively evaluate the OAFlux datasets in the northern of SCS, which will guide the researchers to use OAFlux in a reasonable way in the SCS-related works. Also we find the possible sources of biases that lead to the biases in the heat fluxes, and give some suggestions for the improvement of future observations to improve the credibility of the OAFlux reanalysis dataset. Anyway, we will continue this study, our next research plan is to improve the parameterization scheme in the COARE3.0 bases on the in-suit observations. At last, we will constantly modify the manuscript until it meets the requirements of AMT, and we will strive for an early publication which will make a contribution to SCS-related air-sea interaction research.

Response to SC2#

General Comments

The observation data of this work is new and valuable and provides a further validation in the seasonal variability of the accuracy of OAFlux products in the South China Sea. It seems that the accuracy of OAFlux products varies with the change of prevailing monsoon over the SCS, this is very interesting.
The study found that the OAFlux overestimates (underestimates) U (Qa) throughout the year, and the better estimate were found in winter and spring than in summer and autumn. This should be of essential for the air-sea interaction research community in the South China Sea.

Response: Thanks for your comments on our MS entitled “Evaluation of OAFlux datasets based on in situ air-sea flux tower observations over the Yongxing Islands in 2016”, we have studied your comments carefully and found your comments are very helpful, especially you found out an inconsistent between the Fig.7 and the corresponding description in the paper. We have revised the manuscript according to your comments, and the revised parts were underlined in red. We kindly remind you that the revised manuscript (2nd) is modified based on the revised manuscript (1st) of the first reviewer's opinion.

Response to Specific comments

1. The function/aim of COARE3.0 should be given some more explanations. Why you choose COARE3.0 instead of other method to derive SHF and LHF?

Response: Due to the limited text, there is no specific description of the COARE3.0 algorithm in this paper. Readers can read the following references for more information of COARE3.0 (Fairall et al., 2003; Lisan et al., 2008). Compared to COARE2.5, the updated COARE3.0 has some noted improvements. The range of wind speed validity is now extended to 0–20 ms^{-1} after modifying roughness representation. The transfer coefficients are redefined in terms of conservative quantity rather than the measured quantity, thus eliminating the need for a Webb et al.

(1980) correction to latent heat flux. The COARE 3.0 is shown to be accurate within 5% for wind speeds of 0–10 m s^{-1} and 10% for wind speeds between 10 and 20 m s^{-1}.

There are several forms of bulk flux algorithms currently available (Brunle et al., 2002). The differences between the algorithms reside in the differences in treating the parameterizations of the transfer coefficients C_e and C_h, conditions of light wind and stable stratification, influence of sea spray, treatment of sea state (swell, directional effects), appropriate averaging scales, parameterization of mesoscale gustiness, and the behavior of scalar sublayer transfer. In this paper, the OAFlux reanalysis *SHF* and *LHF* data were calculated by the state-of-the-art COARE bulk flux algorithm version 3.0, in order to avoid the deviation caused by different algorithms in the process of comparison and evaluation, so we also adopted COARE3.0 to derive *SHF* and *LHF* to keep consistent with OAFlux.

2. Authors pointed out that the sea surface temperature Ts is the key variable to determine the differences of sensible heat flux from OAFlux products and in-situ observations. It seems that Ts has better accuracy in winter and spring than in summer and autumn. In Page 8, Line 28-30, author mentioned the influence of cloudy days could be the reason for the inaccuracy of Ts derived from AVHRR and the cloud mount can be related to the outgoing long wave radiation (OLR) shown in Fig. 7. OLR is related to the cloud amount, but as I know that OLR is generally obtained by the satellite remote sensing. It cannot be directly observed by the instrument installed on the flux tower introduced in the paper. Besides, the variable shown in Fig. 7 is downward long wave radiation (DLR), so the content of this part is inconsistent and confusion.

Response: Thank you very much to point out this inconsistent in the text. Actually, at the begging the authors thought that using OLR to infer the cloud cover directly. However, no remote sensing OLR datasets available during this period of observation was found. We used DLR observed from YXASFT to estimate cloud cover indirectly instead of OLR. As we know, DLR is mainly depends on the air temperature, which can be affected by cloud cover. When the sky was covered with large clouds and thick clouds, the probability of rising air temperature will be bigger, which will further increase the DLR. We plotted the curve of observed DLR in fig.7, but forget to modify the corresponding in the article. Thanks again for reading this paper carefully and find this confusion, we are pleased accept your suggestions, and change OLR into DLR in the article.

Response to Minor comments:

1. The abstract is not concise and coherent enough, and needs to be revised.

Response: We have already revised the abstract based on #1 Reviewer's comments. You could read the new abstract from the revised manuscript in the supplement.

2. The authors should adjust the range of X-axis, Y-axis and the regression line in Figs 3c and 3d. Same problem appears in Fig 6, Figs 8-10.

Response: The figures after adjusted were shown on the revised manuscript.

3. Line 21, 'diminish' should be 'were diminished'

Line 21, Definition of 'Ta, U, Qa, Ts' should be given as these variables are first

mentioned in the MS.
Line24, ‘is observed’ should be ‘was observed’
The label of each subset in Figure 1 should be placed in order.
Response: The above mentioned suggestions were accepted and revised in the corresponding place of the article

Response to SC3#

Short Comments

This manuscript evaluates OAFlux datasets using observations collected at an in-situ tower in the SCS in 2016. COARE3.0 algorithm of estimating the SHF and LHF are used to yield the two datasets (OAFlux and YXASFT). Before the comparison between OAFlux and YXASFT, the fluxes of YXASFT from COARE3.0 algorithm were validated by using fluxes from eddy covariance method. Such measurements are rare and valuable. The structure of the manuscript is very good and the content is clear. The results will be valuable for understanding the applicability of OAFlux in the SCS and I recommend publication of the paper. I have only a comment. I suggest authors compare mean variables (30 min averaged wind, temperature and humidity) obtained from the fast response instruments and slow response instruments. They should be unequal during rain. Because the fast response instruments of Campbell Scientific are very sensitive to precipitation and the observations during precipitation are not available. However, the slow response instruments of YXASFT are available during precipitation. The comparison should be useful for validating the data quality of fast response system.

Response: As you mentioned in the short comments, the fast response eddy flux sensors are very sensitive to precipitation and the observations during the precipitation are not available. Yes, we should pay much attention to this problem in ECF's data quality control, the eddy flux measured by ECF during precipitation must be rejected for further comparison and research. However, due to the limitation of scientific research funds, no precipitation observation equipment is installed on the YXASFT, and the eddy flux (SHF and LHF) measured by ECF system was directly used to compare with COARE3.0. So, in the chapter 3.1 of this paper, we illustrated this problem with the description of “A larger difference in the LHF measurement occurs when relatively larger LHF values are observed (e.g., 2016/02/07 and 2016/02/25), which can be readily observed in **Fig. 3a**.The precipitation on these days is the most likely explanation for the overestimation in the LHF by the ECF system (Mauder et al., 2006). Although the YXASFT possesses a lack of field precipitation observations, we can speculate that precipitation may have occurred on 2016/02/07 based on a 1.8℃ drop in the air temperature and an increase of 13% in the relative humidity within the daily mean.”
We accepted your suggestions and compared the mean variables (30 min averaged wind, temperature and humidity) obtained from the fast response instruments and

slow response instruments. As we can see from Fig.1, the two sensors could accurately measure the temperature and wind speed, and both were not affected by the precipitation. But, in term of water vapor observation, the fast response sensor EC150 made by CSI was obviously disturbed by the precipitation, and the data will be seriously polluted. In the period of comparison, four times of possible precipitation was marked by dashed ellipse in Fig.1, the time of four possible precipitation were on 2016/02/03, 2016/02/07, 2016/02/25, 2016/03/26, respectively. Strictly speaking, the ECF data in these four time windows must be eliminated before compared with COARE3.0. In this paper, we didn't eliminate the possible data polluted by precipitation, but it almost does not affect the validation. The LHF comparison between eddy covariance and COARE3.0 (Fig.3) shows a good consistency except for the above mentioned possible precipitation windows. We agree very much that if the ECF data during precipitation days were eliminated, the comparison between CAORE3.0 and ECF will be more consistent, which will further demonstrate the reliability of the COARE3.0 algorithm in SCS. In the next study, we will install the precipitation observation equipment on the YXASFT to improve the reliability of ECF data.

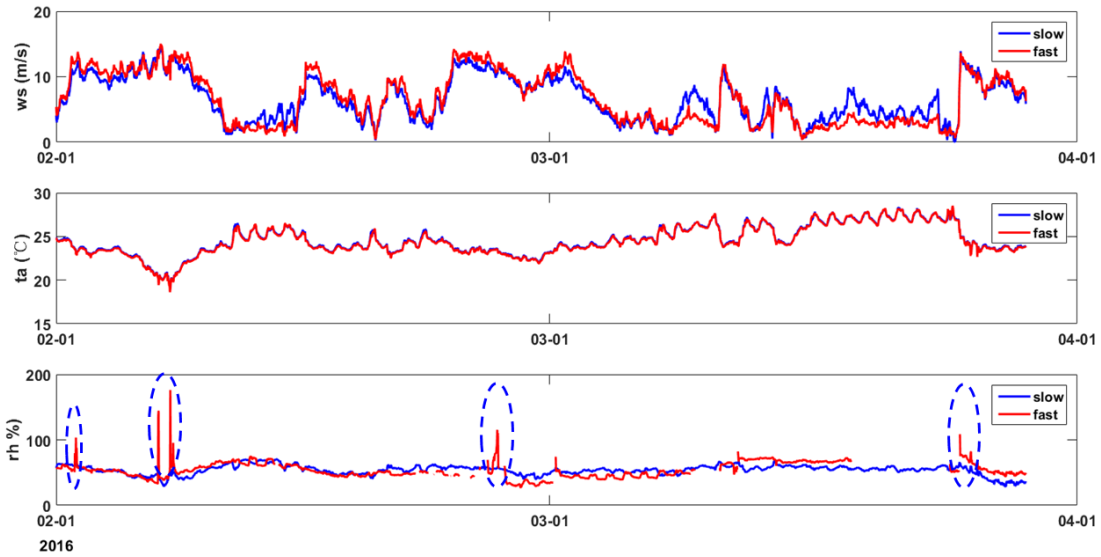

Fig.1 Time series of observed wind speed (ws), air temperature (ta), air relative humidity (rh) by the slow and fast response sensors, respectively. The time windows for possible precipitation were marked by dashed ellipse.

Evaluation of OAFlux datasets based on in situ air-sea flux tower observations over the Yongxing Islands in 2016

Fenghua Zhou[1], Rongwang Zhang[1], Rui Shi[1], Ju Chen[1], Yunkai He[1], Lili Zeng[1], Dongxiao Wang[1*], Qiang Xie[2]

[1]State Key Laboratory of Tropical Oceanography, South China Sea Institute of Oceanology, Chinese Academy of Sciences, Guangzhou 510300, China
[2]Institute of Deep-sea Science and Engineering, Chinese Academy of Sciences, Sanya 572000, China; Laboratory for Regional Oceanography and Numerical Modeling, Qingdao National Laboratory for Marine Science and Technology, Qiangdao, 266237, China

Correspondence to: Dongxiao Wang (dxwang@scsio.ac.cn)

Abstract. The ~~high quality~~ Yongxing air-sea flux tower (YXASFT), which was specially designed for air-sea boundary layer ~~flux-related~~ observations, was constructed on Yongxing Island in the South China Sea (SCS). Surface bulk variable measurements were collected during a one-year period from 2016/02/01 to 2017/01/31. The sensible heat flux (*SHF*) and latent heat flux (*LHF*) were further derived via the Coupled Ocean-Atmosphere Response Experiment version 3.0 (COARE3.0) ~~using those variables~~. This study employed the YXASFT in situ observations to evaluate the Woods Hole Oceanographic Institute (WHOI) OAFlux reanalysis data products ~~in the SCS~~. ~~The study period was divided into the spring, summer_autumn and winter periods to conduct seasonal comparisons for each variable.~~

First, the reliability of COARE3.0 data in the SCS was validated using direct turbulent heat flux measurements via an eddy covariance flux (ECF) system. The *LHF* data derived from COARE3.0 are highly consistent with the ECF ~~measurements~~ with a coefficient of determination (R^2) of 0.78. Second, ~~to conduct seasonal comparisons,~~ the overall reliabilities of the bulk OAFlux variables were diminished in order from T_a (air temperature), U (wind speed), Q_a (air humidity) to T_s (sea surface temperature) based on a combination of R^2 values and biases. OAFlux overestimates (underestimates) U (Q_a) throughout the year and provides better estimates of both variables in the winter and spring than in the summer_autumn period, which seems to be highly correlated with the monsoon climate in the SCS. The lowest R^2 ~~value is observed~~ between the OAFlux-estimated and YXASFT-observed T_s, indicating that T_s is the least reliable ~~product~~ dataset and should thus be used with considerable caution. In terms of the heat fluxes, OAFlux considerably overestimates *LHF* with an ocean heat loss bias of 52 w/m^2 (73% of the observed mean) in the spring, and the seasonal OAFlux *LHF* performance is consistent with U and Q_a. The OAFlux-estimated *SHF* appears to be poorly representative with enormous overestimations in the spring and winter, while its performance is much better during the summer_autumn period. Third, ~~an~~ analysis reveals that the biases in Q_a are the most dominant factor on the *LHF* biases in the spring and winter and that the biases in both Q_a and U are responsible for controlling the biases in *LHF* during the summer_autumn period. The biases in T_s are responsible for controlling the *SHF*

带格式的：字体：（默认）+西文正文 (Times New Roman)

biases, and the effects of biases in T_s on the biases in *SHF* during the spring and winter are much greater than that in the summer_autumn period.

1 Introduction

Exchanges of momentum, heat and water vapor fluxes at the air-sea interface constitute a significant component of air-sea interactions, which affect weather processes and climate change at all scales (Zhu et al., 2002; Persson et al., 2002; Frenger et al., 2013). As the surface that lies beneath the atmosphere, the ocean influences the stability of the atmospheric layer and the evolution of the atmospheric boundary layer through turbulent exchange (Chelton and Xie, 2010). ~~For example, the water vapor supplied by latent heat transport can determine the regional and even global precipitation (de Cosmo et al., 1996).~~ In addition, sensible heat flux (*SHF*) and latent heat flux (*LHF*) at the air-sea interface are both important factors that affect changes in the mixing layer and thermocline (Hogg et al., 2009).

Accurate calculations of ~~regional and global~~ air-sea fluxes play a crucial role in driving marine and atmospheric circulation models, understanding atmosphere-ocean interactions, and evaluating and assessing numerical weather forecast models (Sun et al., 2003). Currently available air-sea flux datasets (including satellite remote sensing inversion data and reanalysis data) are quite uncertain, as they are mainly derived from inaccurate flux modeling algorithms and uncertainties in the turbulent exchange coefficient were also involved in the fluxes calculations ~~uncertainties in the measured values of basic observational quantities involved in the calculation of fluxes~~ (Zeng et al., 1998; Josey, 2001; Smith et al., 2001). In turn, these intrinsic uncertainties limit the ability to assess numerical models based on flux datasets (Yu et al., 2006). ~~Thus, the appropriate evaluation of a flux dataset is necessary prior to use them in specified study sea area.~~

The South China Sea (SCS) is mainly controlled by various monsoon systems~~.~~; it is connected with the western Pacific Ocean and the Indian Ocean through marine and atmospheric processes, and thus, the SCS exhibits potential influences on global climate change as well as regional climate regimes (Wang et al., 2006; Shi et al., 2015). Air-sea interactions in the SCS induce many marine meteorological hazards and greatly affect the transfer of heat and water vapor in regions throughout South China and Southeast Asia (Yang et al., 2015). Acquiring long-term observations of air-sea fluxes in the SCS can therefore help us to better understand the characteristics and evolutionary behavior of air-sea interactions in the SCS, optimize the parameterization schemes in atmospheric models, and improve long-term weather forecasts and extreme hazardous weather alerts.

To achieve the abovementioned scientific goals, a mesoscale observation network in the Xisha sea area in the northern SCS was initiated in 2008 (Yang et al., 2015) with the primary ambition of researching air-sea interactions. At present, the observation network includes a surface mooring buoy array, a system of shore-based wave-tide gauges, an automatic weather station, a shore-based boundary layer air-sea flux tower

带格式的：字体：倾斜
带格式的：字体：倾斜
带格式的：正文
带格式的：字体：10 磅，英语(美国)
带格式的：字体：10 磅
带格式的：正文
带格式的：字体：10 磅，英语(美国)
带格式的：字体：10 磅

~~a shore-based air-sea boundary flux tower~~, and a submerged mooring buoy array. A large dataset comprising in situ observational data was obtained to serve as "ground truth" reference data to quantify the uncertainties within regional model flux products for the SCS.

Many in situ observations and model analysis comparisons have been studied in different oceans around the world, including the Arabian Sea (Weller et al., 1998; Swain et al., 2009), the tropical Pacific Ocean (Weller and Anderson, 1996; Wang and McPhaden, 2001), the northeast Atlantic Ocean (Sun et al., 2003; Yu et al., 2004), the Indian Ocean (Goswami, 2003) and the SCS (Zeng et al., 2009; Wang et al., 2013). ~~Among the world's oceans, the SCS is unique in that it is dominated by seasonally reversing monsoon winds, including those of the northeast and southwest monsoons.~~ Unfortunately, due to limited field observations of flux-related variables, detailed evaluation studies in the SCS are scarce.

In this study, turbulent *SHF* and *LHF* variations as well as numerous bulk variables, including the air temperature (T_a), sea surface temperature (T_s), air humidity (Q_a) and wind speed (U), from the Woods Hole Oceanographic Institution (WHOI) Objectively Analyzed Air-Sea Fluxes (OAFlux) project are compared with ~~high-quality tower-based~~YXASFT measurements ~~collected from the Yongxing Islands throughout~~in the northern SCS. This investigation spans a full year from 2016/02/01 to 2017/01/31. Seasonal comparisons of the bulk variables and heat fluxes are described in **Sect. 3**. An overview of the instrumentation on the Yongxing air-sea flux tower (YXASFT) in addition to the data and methodology employed in this paper are introduced in **Sect. 2**. Finally, the summary and conclusions are provided in **Sect. 4**.

带格式的：字体：倾斜

带格式的：字体：倾斜

2 Instrumentation, data and methods

2.1 Yongxing air-sea flux tower (YXASFT)

The 20-m-tall YXASFT **(Fig. 1a),** which was specially designed for the observation of air-sea boundary layer fluxes, is located approximately 100 m off the northeastern coastline of Yongxing Island (16.84 °*N*, 112.33 °*E*; **Fig.** ~~**2**~~**1d**~~**b**~~ **and** ~~**2d**~~**1e**). A gradient meteorological system (GMS) and an eddy covariance flux (ECF) system were mounted on the tower **(Fig.** ~~**1c**~~**1b)**. A CR3000 data logger manufactured by Campbell Scientific Company, USA, is used for data sampling, preprocessing, storage, and transmission. The real-time observation data from the YXASFT are open for access at the website http://mabl.scsio.ac.cn:8040 (login: CSL-CER and password: ruhuna). A data sharing agreement must be signed by the user before ~~the data can be downloaded~~being authorized to download the data.

The sensor wiring and data acquisition diagram for the YXASFT is shown in **Fig. 2**. The observational variables within the GMS include U, the wind direction (W_d), T_a, Q_a, the air pressure (P_a), the net radiation (R_n) and T_s. Each parameter is sampled once every second, and 1-, 10- and 30-min averages are recorded and transmitted to the data center in real-time. The ECF system can collect high-frequency turbulent data with a 10-Hz sampling frequency. Successive 30-min fully corrected fluxes of the momentum (T_{au}), *SHF*, *LHF*, and CO_2 (F_c) can be calculated using the online program Easy_flux. The sensors in the YXASFT and their respective measurement specifications are listed in **Table 1**. All of the sensors **(Fig. 1ce)** have been checked via pre- and post-installment calibrations by the National Center of Ocean Standards and Metrology.

2.2 Data

The data employed in this study originate from two sources. The in situ observations obtained by YXASFT" ~~The in-situ datasets comprise observations from the sensors on the YXASFT~~, and the reanalysis datasets are derived from the OAFlux project. Table 2 shows various information, including the variable height, time period, data interval and data location, regarding the data adopted in this study.

2.2.1 *In situ* data

High-frequency turbulent data (u, v, w, t, ρ_v) were collected by the ECF system installed at a height of 12 m from 2016/02/01 to 2016/03/29. Direct measurements of turbulent data were further used to calculate the fluxes using the eddy covariance (EC) method in a specified time period (30 min or 60 min). Meanwhile, direct measurements of turbulent fluxes using the ECF system were used only to verify the applicability of version 3.0 of the Coupled Ocean-Atmosphere Response Experiment (COARE3.0) over the SCS.

The selected 30-min averages of the bulk variables (U measured at a height of 10 m and T_a, Q_a and T_s measured at a height of 5 m) used for the bulk flux calculations range from 02/01/2016 to 01/31/2017. Note that T_s was measured using an SI-112 infrared radiation thermometer manufactured by Campbell Scientific Company, USA, installed at a height of 5 m, and therefore, we consider T_s as representative of the sea surface temperature at a depth of 0.05 m. The value of Q_a was derived using **Eq. 1** as described in COARE3.0 using T_a, the relative humidity (R_h) and the air pressure (P_a). Furthermore, this paper also adopts *SHF* and *LHF* averages within 30-min intervals derived via COARE3.0 using the input observed bulk ~~parameters~~variables. The ~~measurement~~ heights of T_a and Q_a in the OAFlux dataset are both 2 m, while the measurement heights for these two parameters on the YXASFT are both 5 m. Thus, prior to conducting a comparison, we corrected the corresponding heights of the in situ data to correspond to the ~~variable~~ heights in the OAFlux dataset using COARE3.0. In addition, downward longwave radiation (*DLR*) data measured using an NR01 net radiometer manufactured by Hukseflux, Netherlands were used in this paper as an indirect variable to infer the cloud cover in the sky.

$$e_s = 6.112e^{\frac{17.502T_a}{T_a+240.97}(1.0007+3.46P_a*10^{-6})}$$
$$Q_a = \frac{621.97e_s}{(P_a-0.378)R_h/100} \quad (1)$$

2.2.2 Reanalysis data

In this paper, the OAFlux reanalysis data were selected for two reasons. First, a previous study showed that the OAFlux dataset is the most preferable among five different products (i.e., ERA-1, NCEPS, JRA55, TropFlux and OAFlux) with regard to *LHF* data over the SCS (Wang et al., 2017). Second, OAFlux represents the most recently updated data product (as of July 2017) accessible for the study period. OAFlux is an ongoing global flux product compiled by WHOI with a spatial

带格式的：字体：10 磅，英语(美国)
带格式的：正文
带格式的：字体：10 磅
带格式的：字体：非加粗
带格式的：字体：（默认）Times New Roman，（中文）+中文正文（宋体），字体颜色：自动设置，（中文）中文(中国)，（其他）英语(美国)，图案：清除

resolution of 1°x1°. OAFlux utilizes an integrated analysis method to combine satellite data with modeling and reanalysis data, and it employs COARE3.0 to calculate heat fluxes (Yu et al., 2008). In this study, the daily mean OAFlux datasets include U, Q_a, T_s, T_a, LHF and SHF, and YXASFT observations during the same time period were used for a comparison.

2.3 Methods

2.3.1 Bulk algorithm

The bulk algorithm utilized in this study is based on the Monin-Obukhov similarity theory, which is widely considered to be an advanced bulk algorithm (Fairall et al., 1996). To keep consistent with the bulk method of calculating flux in OAFlux, ~~The latest bulk flux algorithm in~~ the COARE3.0 was used to calculate the heat fluxes using the in-suit observation bulk parameters ~~at the air-sea interface~~ in this paper. Compared to COARE2.5, the updated COARE3.0 has some noted improvements as follows. First, the range of wind speed validity is now extended to 0–20 m/s after modifying roughness representation. Second, the COARE 3.0 is shown to be accurate within 5% for wind speeds of 0–10 m/s and 10% for wind speeds between 10 and 20 m/s~~To date, this method has achieved reliable calculation accuracies in the wind speed range of 1-10 m/s and has made great progress with regard to heat flux calculation accuracies at high wind speed conditions~~ (Fairall et al., 2003). In this method, the calculation equations for the SHF and LHF can be written as follows:

$$SHF = \rho_a C_p C_h U (T_s - T_a) \tag{2}$$

$$LHF = \rho_a L_e C_e U (Q_s - Q_a) \tag{3}$$

where ρ_a represents the air density, L_e represents the latent heat of evaporation, C_p represents the constant-pressure specific heat, U represents the sea surface wind speed (measured at a height of 10 m in this study), C_e and C_h correspond to the turbulence exchange coefficients for the latent heat and sensible heat, respectively, Q_s and Q_a correspond to the air saturation specific humidity at the sea surface and the air specific humidity near the sea surface, respectively, and T_s and T_a correspond to the sea surface skin temperature and the air temperature near the sea surface, respectively. In **Eqs. 2** and **3**, only U, T_s, T_a and Q_a are independent measurement variables, while the remainder of the variables must be calculated based on the four independent variables.

2.3.2 Eddy covariance method

The EC method is one of the most direct ways to measure and calculate turbulent fluxes (Crawford et al., 1993). Reynolds decomposition is utilized to break raw data down into their means and deviations. Furthermore, the values of SHF and LHF can be calculated as the covariances between w and scalar values (t, ρ_v) using the following formulas, respectively:

$$SHF = \rho C_p \overline{w't'} \tag{4}$$

$$LHF = \lambda \overline{w'\rho_v'} \tag{5}$$

where ρ is the dry air density, C_p is the specific heat of dry air at a constant pressure (where 1004.67 $Jkg^{-1}K^{-1}$ is used in the calculation), and λ is the latent heat ratio of water vapor evaporation. The overbar represents the Reynolds–ensemble average, and the prime symbol denotes the instantaneous deviation from the ensemble average.

2.3.3 Data processing

To match the timescale of the OAFlux daily data, we derived the daily means of the YXASFT-observed bulk variables and heat fluxes by averaging all of the 30-min datasets from each day. In addition, we used bilinearly interpolated OAFlux values (inversely weighted by the distance) from the surrounding four grid points (111.5 °*E*, 16.5 °*N*; 112.5 °*E*, 16.5 °*N*; 112.5 °*E*, 15.5 °*N*; 111.5 °*E*, 15.5 °*N*) to represent the corresponding OAFlux value at the YXASFT observation site.

The comparison between the YXASFT and OAFlux datasets (described in **Sects. 3** and **4**) was quantitatively analyzed by using the mean bias (*Bias*, defined in **Eq. 6**), root mean squared error (*RMSE*, defined in **Eq. 7**), coefficient of determination (R^2) and linear regressions, respectively.

$$Bias = \frac{1}{N}\sum_{i=1}^{N}(x_i - y_i) \tag{6}$$

$$RMSE = \sqrt{\frac{1}{N}\sum_{i=1}^{N}(x_i - y_i)^2} \tag{7}$$

where x and y denote the OAFlux values and YXASFT observations, respectively.

3 Results and discussion

3.1 Validation of COARE3.0 using direct ECF measurements

The heat fluxes from both YXASFT and OAFlux used for the comparison herein were derived from COARE3.0. However, the COARE algorithm was originally developed for the Tropical Ocean Global Atmosphere-COARE (TOGA-COARE) experiment in tropical oceans (Fairall et al., 1996), while the reliability of COARE3.0 was verified by (Brunke et al., 2003) using 12 ship cruises over tropical and mid-latitude oceans (between 5 °*S* and 60 °*N*). The adaptability of OAFlux in the SCS must ~~ yet~~ be verified due to its unique geographical location (i.e., it is the largest marginal sea in the northwestern Pacific Ocean) and its monsoon climate system. In this study, the EC fluxes directly measured using the IRGASON ECF system manufactured by Campbell Scientific, USA, were used to validate the performance of COARE3.0 in the SCS.The EC method is mathematically complex, significant care is required to set up different processing steps for different sites, measurements and study purposes. In this paper, the EC program running on CR3000 was based on the processing steps shown in **Fig. 3**. The daily LHF time series in COARE3.0 are basically consistent with those in ECF **(Fig. ~~3a~~4a)** with an R^2 value of 0.78 (**Fig. ~~3c~~4c**). COARE3.0 underestimates the *LHF* with a mean bias of 18.55 w/m^2 (19.9% of the ECF mean) relative to direct ECF observations. A larger difference in the *LHF* measurement occurs when relatively larger *LHF* values

带格式的：字体：10 磅
带格式的：字体：10 磅
带格式的：字体：10 磅
带格式的：字体：10 磅
带格式的：字体：10 磅，英语(美国)
带格式的：字体：10 磅
带格式的：字体：倾斜
带格式的：字体：倾斜
带格式的：字体：倾斜

are observed (e.g., 2016/02/07 and 2016/02/25), which can be readily observed in **Fig. ~~3a~~4a**. The precipitation on these days is the most likely explanation for the overestimation in the *LHF* by the ECF system (Mauder et al., 2006; zhang et al., 2006). Although the YXASFT possesses a lack of field precipitation observations, we can speculate that precipitation may have occurred on 2016/02/07 based on a 1.8 ℃ drop in the air temperature and an increase of 13% in the relative humidity within the daily mean. In addition, we spot similar trends on 2016/02/25. In contrast, the *SHF* data pair is far from agreement with an R^2 value of 0.03 (**Fig. ~~3d~~4d**). The large variation in the *SHF* observed using the ECF is not detected within the COARE3.0-derived time series (**Fig. ~~3b~~4b**). Direct heat flux measurements with a 60-day interval obtained using the ECF system show that *SHF* (with a mean value of 23.5 w/m^2) is significantly smaller than *LHF* (with a mean of 93.3 w/m^2). A small *SHF* magnitude may amplify variations in the time series and reduce the R^2 values in scatter plots under the same deviation values. In this comparison, we were more concerned about the magnitude of correlation in the *LHF* data. Thus, COARE3.0 was considered to be receptive and was used as an appropriate bulk flux algorithm over the SCS.

带格式的：字体：倾斜

带格式的：字体：倾斜

3.2 Evaluation of the OAFlux datasets

OAFlux is a flux product based on a composite algorithm that improves the calculation accuracies of flux-related variables by using a weighting method for target analysis. However, this method could lead to a time-scale mismatch if the data variables have different data sources (Fairall et al., 2010). It is therefore necessary to evaluate the OAFlux dataset to assess its applicability in the SCS before further application. ~~.~~

带格式的：检查拼写和语法

带格式的：字体：（中文）Times New Roman

3.2.1 Time series of the YXASFT observations and OAFlux reanalysis data

Time series of the bulk variables and heat fluxes are given in **Figs. ~~4~~ 5** and **~~5~~6**, respectively. As shown in **Fig. ~~5~~6**, there is an obvious overestimation in both *SHF* and *LHF* in OAFlux compared with the YXASFT observations, and this overestimation demonstrates an evident seasonal variation. The time series of *LHF* from the YXASFT observations and OAFlux data show essentially consistent variation trends and agree with one another better during the spring (February to March) and winter (December to January) than during the summer and autumn (April to November) (**Fig. ~~5b~~6b**). The *SHF* variation trend appears to be opposite to that of *LHF*, since the deviations during the winter and spring are clearly larger than those during the summer and autumn (**Fig. ~~5a~~6a**). For the bulk variables in **Fig. ~~4~~5**, the OAFlux data maintained a higher consistency with the YXASFT observations with regard to the overall variation trend. Furthermore, U and Q_a seemed to match better during the winter and spring periods, while an overestimation (underestimation) in U (Q_a) is more evident during the summer and autumn periods (**Fig. ~~4a~~ 5a** and **~~4b~~5b**). Some abrupt drops (i.e., variations of 3 to 5 days) in the YXASFT T_s observations were obviously not captured by OAFlux (**Fig. ~~4d~~5d**). In the next section, we divide the annual study period into three periods, namely, spring (2016/02/01-2016/03/31), summer_autumn (2016/04/01-2016/11/31) and winter (2016/12/01-2017/01/31), to conduct a detailed comparison of their seasonal variations.

3.2.2 Comparison of the bulk variables

The heat fluxes from both OAFlux and YXASFT were derived using COARE3.0. Thus, we can further analyze the origin of the seasonal deviations in the heat fluxes by conducting seasonal comparisons of the bulk variables. The scatter plots of U, Q_a, T_s, and T_a constructed using the YXASFT and OAFlux data for the three separate periods are shown in **Fig. ~~6~~7**, and a quantitative statistical summary for each variable is listed in **Table 3**.

U: The spring, summer_autumn, and winter periods in the Yongxing Islands represent the monsoon transition, southwest monsoon and northeast monsoon periods, respectively. Previous studies indicated that the northeast monsoon in the northern SCS is much stronger than the southwest monsoon (Yan et al., 2005). In this study, the observed mean wind speeds during the three periods were 6.40, 4.97 and 9.40 m/s. It can be seen from **Fig. ~~6~~7 (first row)** that the R^2 values of U between the OAFlux and YXASFT data during the three periods are 0.90, 0.79 and 0.92. OAFlux overestimates the values of U in the spring, summer_autumn, and winter periods with mean biases of 0.96 (15% of the YXASFT-observed mean value), 1.19 (24%) and 0.67 m/s (7%), respectively.

Q_a: The southwest monsoon is often accompanied by a high water vapor and cloudy skies (Chen et al., 2012). Therefore, the Q_a value during the summer_autumn period was the highest throughout the year with an observed mean of 21.08 g/kg. The R^2 values of Q_a between the OAFlux and YXASFT data during the three periods are 0.81, 0.68 and 0.80 (**Fig. ~~6~~7 (second row)**). In contrast to U, OAFlux exhibits an overall underestimation of Q_a in the spring, summer_autumn, and winter periods with dry biases of 0.33 (2%), 0.75 (4%) and 0.11 g/kg (1%), respectively.

T_a: The OAFlux T_a values are highly consistent with the YXASFT observations with R^2 values of 0.92, 0.84 and 0.89 in the spring, summer_autumn, and winter periods, respectively (**Fig. ~~6~~7 (fourth row)**). As shown in **Fig. ~~4c~~5c**, both the seasonal trends and day-to-day variations are effectively captured in the OAFlux data. The OAFlux reanalyzed T_a data have a warmer bias of 0.52 ℃ (2%) in the spring and colder biases of 0.10 (0.3%) and 0.57 ℃ (2%) in the summer_autumn and winter periods, respectively. Consequently, the OAFlux-estimated T_a can be considered as the most reliable variable in this study.

T_s: The OAFlux-estimated T_s captures only the seasonal trend, and the estimates exclude some special synoptic signals, such as abrupt drops during cold air temperatures and typhoons or gradual temperature increases induced by the passage of a warm eddy. The R^2 values of T_s between the OAFlux and YXASFT data are relatively small when compared with those of U, Q_a and T_a, suggesting that the reliability of the OAFlux-analyzed T_s is generally low. In contrast to U and Q_a, the OAFlux T_s performance better in the summer_autumn period (R^2=0.70) than in the spring (R^2=0.47) and winter (R^2=0.54) periods, as shown in **Fig. ~~6~~7 (third row)**.

In summary, the seasonal performances of the OAFlux-estimated U and Q_a seem to be highly correlated with the monsoon system in the SCS. This manifests a better performance of the OAFlux-estimated U (Q_a) during the spring and winter periods characterized by a stronger (drier) northeast monsoon than during the summer_autumn period characterized by a relatively weaker (wetter) southwest monsoon. The significant difference between the T_s estimates may stem largely from the fact that the OAFlux T_s estimates are retrieved using the Advanced Very High Resolution Radiometer (AVHRR), which is easily affected by the presence of clouds. Therefore, the available OAFlux T_s estimates were dramatically reduced during the

abovementioned special synoptic processes. With the onset of the southwest monsoon, the average total cloud cover, low cloud cover and precipitation all increase throughout the SCS (Yan et al., 2003), and the T_s retrieved via the AVHRR should correspondingly exhibit a lower quality. However, this trend is not observed in the results of this paper. We further utilized in situ observations of the downward longwave radiation (*DLR*)~~outgoing longwave radiation (*OLR*)~~ to infer the sky cloud cover. There is an evidently greater fluctuation in the ~~*OLR*~~ *DLR* during the winter and spring periods than in the summer_autumn period, indicating that the winter and spring seasons possess greater probabilities of cloudy days (**Fig. ~~7~~8**). This interesting phenomenon may be caused by the fact that the intensity of the summer monsoon in 2016 was weaker than those in preceding years; this hypothesis will be further explored hereafter.

3.2.3 Comparison of heat fluxes

The scatter plots of the *LHF* and *SHF* estimates obtained from the YXASFT and from OAFlux during the three periods are shown in **Fig. ~~8~~9**, and a quantitative statistical summary of each variable is also listed in **Table 3**. Note that an upward (downward) heat flux is positive (negative) in this paper, and a positive (negative) value represents the loss (gain) of ocean heat to (from) the atmosphere.

LHF: Compared with the YXASFT observations, the OAFlux-estimated *LHF* is overestimated by a mean bias of 50.95 (70%) in the spring, 42.43 (76%) in the summer_autumn and 63.29 w/m^2 (74%) in the winter. The R^2 values are 0.80 in the spring, 0.66 in the winter and 0.40 in the summer_autumn (**Fig. ~~8~~ 9 (first row)**). This is also consistent with the R^2 values for U and Q_a, which are the two key input factors in the *LHF* calculations.

SHF: Large *SHF* variations during the spring and winter are not evident in the YXASFT-derived *SHF* time series (**Fig. ~~4e~~5e**). Compared to *LHF*, the OAFlux-estimated *SHF* has the smallest R^2 values for all three individual periods, as shown in **Table 3** for the spring (0.01), summer_autumn (0.31) and winter (0.14). In comparison, the OAFlux-estimated *SHF* is more reliable during the summer_autumn with a mean bias of 1.07 w/m^2 than in the spring (16.83 w/m^2) or winter (23.56 w/m^2).

Overall, we can infer that the OAFlux-estimated *LHF* product is more reliable during the spring and winter periods than during the summer_autumn period, which is consistent with the key input variables U and Q_a, and that the product is further affected by the monsoon system in the SCS. Meanwhile, the *SHF* estimates exhibit opposite characteristics relative to those of *LHF*, as the OAFlux *SHF* product is more credible during the summer_autumn than during the spring and winter periods, which is consistent with the seasonal OAFlux T_s performance and is highly correlated with the cloud cover.

3.3 Possible effects of bulk variables on the biases in the *SHF* and *LHF*

The values of *SHF* and *LHF* were calculated using **Eqs. 2** and **3**. Thus, possible biases in the *LHF* and *SHF* results are mainly associated with the input bulk variables and the parameterization of the turbulent exchange coefficients in the equations. In this paper, the parameterization scheme is not discussed due to limited space. The relationships among the OAFlux *LHF* bias with U, Q_a and T_s were studied extensively by a previous study through years of moored buoy data, automatic weather station (AWS) data and cruise data over different regions in the SCS; it was found that the biases in Q_a dominated the *LHF* biases, followed by the biases in U (Wang et al., 2017). To determine whether similar conclusions exist

带格式的：字体：倾斜

带格式的：字体：倾斜

in this study and to quantify the relationships among the heat flux biases and the bulk variable biases, we constructed scatter plots of the biases in *LHF* (**Fig. ~~9~~10**) and *SHF* (**Fig. 1~~0~~0**) against the biases in *U*, Q_a, T_s and T_a. All of the biased data were normalized first to understand their relative importance.

ΔLHF: The biases in Q_a are the most dominant factor in determining the biases in *LHF* during the spring ~~and winter~~ with relatively high R^2 values of 0.38 ~~in the spring and 0.43 in the winter~~ compared with the other biased bulk variables (**Fig. ~~8~~ 10 (first ~~and third~~ column~~s~~)**). Both of the Q_a and *U* biases are responsible for controlling the biases in *LHF* during the summer_autumn period with R^2 values of 0.36 and 0.32, respectively (**Fig. ~~8~~ 10 (second column)**). Both of the Q_a and T_a biases are the dominate factors in determing the biased in LHF during the winter period with R^2 values of 0.43 and 0.16, respectively (**Fig. 9 (third column)**). ~~Both of t~~The biases in T_s ~~and T_a are~~is negligible control factors on the biases in *LHF*, since their R^2 values are all relatively small during the three periods compared with those of Q_a (**Fig. ~~8~~ 9 (third and fourth rows)**). In general, the result revealed that the Q_a is the most dominated factor controlling the biases in *LHF* throughout the year is similar to those reported in previous studies ~~SCS~~ (Wang et al., 2013, 2017). Additional, these dominate factors that cause the seasonal biases in LHF are new findings in this article.~~These results reveal effects of biased bulk parameters on the biases in *LHF* similar to those reported in previous studies for the SCS (Wang et al., 2013, 2017).~~

ΔSHF: During the observational period, the biases in T_s were the key factor dominating the biases in *SHF*. The effects of T_s biases on the biased *SHF* during the spring (R^2=0.79) and winter (R^2=0.72) periods were much larger than that during the summer_autumn period (R^2=0.38), which is also consistent with the fact that OAFlux better estimates T_s in the summer_autumn than in the spring ~~or~~ and winter (**Fig. ~~6~~ 7 third row**). From **Eq. 2**, *SHF* is largely determined by T_s-T_a, as shown in **Fig. ~~5~~6**. OAFlux is unable (able) to capture the variations in T_s (T_a) during the spring and winter, thereby causing large fluctuations in T_s-T_a and further leading to large variabilities in the OAFlux *SHF* time series.

带格式的：字体：非倾斜

带格式的：非上标/ 下标

4 Summary and conclusions

Successive air-sea heat flux-related observational data were acquired over the course of a year (2016/02/01-2017/01/31) at the YXASFT in the Yongxing Islands. In this paper, we first used direct heat flux measurements from a high-frequency (10 Hz) ECF system to validate the reliability of the COARE3.0 bulk algorithm in the SCS. Then, seasonal comparisons were conducted for the daily mean surface bulk variables and heat fluxes between the WHOI OAFlux products and YXASFT observations. Finally, the effects of biased bulk variables on the biases in the heat fluxes were presented to determine the possible sources of the biases in *LHF* and *SHF*. The conclusions are summarized as follows.

The magnitude of the mean of the directly measured *SHF* is small compared with that of *LHF* and can even be ignored in air-sea heat flux interactions during the ECF measurement period. Therefore, we were more concerned with the *LHF* estimation differences between COARE3.0 and the ECF system in this validation. The daily mean *LHF* from COARE3.0 was basically consistent with the ECF measurements with a high R^2 and an acceptable bias. Furthermore, if possible

precipitation periods were excluded, the consistency between the COARE3.0 and ECF *LHF* data were better. Thus, the COARE3.0 bulk algorithm was considered to be reliable in this study.

Comparisons of the bulk variables revealed that the reliabilities of the OAFlux datasets diminished in order from T_a, U, Q_a to T_s based on a combination of R^2 values and biases. The performances of the OAFlux-estimated U and Q_a seem to be highly correlated with the monsoon system in the SCS; OAFlux provides a better estimation of U (Q_a) in the spring and winter characterized by a stronger (drier) northeast monsoon than in the summer_autumn characterized by a relatively weaker (wetter) southwest monsoon. Similar to a previous study, this study also indicated that T_s is the least reliable OAFlux product (Sun et al., 2003). The T_s signals during special synoptic process were poorly captured by OAFlux due to the presence of clouds, which affect the recorded AVHRR data. The performance of the OAFlux-estimated T_s is better during the summer_autumn than in the winter or spring due to a reduced cloud cover during the summer monsoon period, which could be attributable to the fact that the summer monsoon in 2016 was weaker than those in preceding years. With respect to a comparison of the heat fluxes, OAFlux considerably overestimates *LHF* with ocean heat loss biases of 50.95 w/m^2 (70%) in the spring, 42.43 w/m^2 (76%) in the summer_autumn and 63.29 *w/m*^{2} (74%) in the winter. Consistent with the key input variables U and Q_a, the OAFlux *LHF* performance is better during the spring and winter than in the summer_autumn, which is further associated with the monsoon climate in the SCS. The seasonal *SHF* reliability is coincident with that of T_s, as the most poorly reliable T_s estimates lead to the most unreliable *SHF* estimates with enormous overestimations throughout the year. An analysis of the possible sources of biases in the heat fluxes show that biases in Q_a are the most dominant factor in determining the biases in *LHF* during the spring and winter. Meanwhile, both of the biases in Q_a and U are responsible for controlling the biases in *LHF* during the summer_autumn period. Biases in T_s are responsible for controlling the biases in *SHF*, and the effects of biases in T_s on the biases in *SHF* during the spring and winter are much greater than that in the summer_autumn period.

In summary, both *Ts* and *SHF* in OAFlux ~~estimates of both T_s and *SHF* using OAFlux~~ should be utilized with considerable caution in further research~~, including driving regional ocean models for the SCS.~~ Additionally, U, Q_a and *LHF* should be used with proper consideration due to their seasonal reliability variations. Researchers should feel more at ease using these data during the northeast monsoon than in the southwest monsoon. The performance of the OAFlux-estimated T_a seems to change little with the seasons and is highly consistent with the YXASFT observations throughout the year. Improving the observation capability of the AVHRR sensor under cloudy conditions is necessary for improving the accuracy of T_s estimates and the reliability of calculating *SHF*. Larger quantities of in situ bulk variable observations and direct turbulent heat flux measurements as well as improvements in the parameterization of variables in different regions of the SCS are also essential for improving the reliability of OAFlux datasets in the SCS.

带格式的：字体：10 磅

带格式的：字体：10 磅

Author contribution

Fenghua Zhou designed the experiments and Rui Shi, Ju Chen and Yunkai He carried them out. Fenghua Zhou and Rongwang Zhang write the Matlab program and performed the data processing and analysis. Lili Zeng and Dongxiao Wang give help on useful discussions and data collection. Fenghua Zhou and Qiang Xie prepared the manuscript with contributions from all co-authors.

Competing interests

The authors declare that they have no conflict of interest

Acknowledgements

This study was funded by the National Natural Science Foundation of China (41706102), the Chinese Academy of Sciences (CAS) Key Technology Talent Program of 2016, the Station Network Construction Project-Xisha Marine Observatory of the CAS (KZCX2-YW-Y202), and the Strategic Priority Research Programs of the CAS (XDA11010302 and XDA11010403). The YXASFT data were provided by the Xisha Deep Sea Marine Environment Observation Station, South China Sea Institute of Oceanology, CAS. All of the in situ data adopted in this study can be obtained by contacting the first author, Fenghua Zhou (zhoufh@scsio.ac.cn). The authors would like to express their gratitude for the reanalysis data products comprising global ocean heat flux and evaporation data provided by the WHOI OAFlux project (http://oaflux.whoi.edu) funded by the NOAA Climate Observations and Monitoring (COM) program. The source code for the COARE 3.0 algorithm is freely available at http://coaps.fsu.edu/COARE/flux_algor/. The first author would like to thank the engineers from Campbell Scientific Company, USA, for their help with the observation system integration and data acquisition on the YXASFT. Finally, the authors thank the anonymous reviewers for their valuable comments and suggestions that improved the quality of this paper.

References

Brunke, M. A., Fairall, C. W., Zeng, X., Eymard, L., and Curry, J. A.: Which bulk aerodynamic algorithms are least problematic in computing ocean surface turbulent fluxes?, J. Climate, 16, 619-635, doi:10.1175/1520-0442(2003)016<0619:WBAAAL>2.0.CO;2, 2003.

Campbell Scientific, Inc. 2018: CR3000 Micrologger, User's Manual. Accessed 21, March 2018, https://s.campbellsci.com/documents/us/manuals/cr3000.pdf.

Chelton, D. and Xie, S.-P.: Coupled Ocean-atmosphere interaction at oceanic mesoscales, Oceanography, 23, 52–69, doi:10.5670/oceanog.2010.05, 2010.

带格式的：字体：（中文）Times New Roman，10 磅

带格式的：缩进：左侧：0 厘米，悬挂缩进：7.2 字符

带格式的：字体：（中文）Times New Roman，10 磅

带格式的：字体：10 磅

带格式的：字体：10 磅

Chen, J., Zuo, T., and Wang, H.: Variation of latent heat flux over the Bengal Bay-South China Sea area and its relationship with South China Sea summer monsoon onset, in: IEEE International Geoscience and Remote Sensing Symposium, Munich, Germany, 22–27 July 2012, 856–859, 2012.

Crawford, T. L., McMillen, R. T., Meyers, T. P., and Hicks, B. B.: Spatial and temporal variability of heat, water vapor, carbon dioxide, and momentum air-sea exchange in a coastal environment, J. Geophys. Res., 98, 12869–12880, doi:10.1029/93jd00628, 1993.

de Cosmo, J., Katsaros, K. B., Smith, S. D., Anderson, R. J., Oost, W. A., Bumke, K., and Chadwick, H.: Air-sea exchange of water vapor and sensible heat: the Humidity Exchange Over the Sea (HEXOS) results, J. Geophys. Res., 101, 12001–12016, doi:10.1029/95jc03796, 1996.

Fairall, C. W., Bradley, E. F., Rogers, D. P., Edson, J. B., and Young, G. S.: Bulk parameterization of air-sea fluxes for tropical ocean-global atmosphere coupled-ocean atmosphere response experiment, J. Geophys. Res., 101, 3747–3764, doi:10.1029/95jc03205, 1996.

Fairall, C. W., Barnier, B., Berry, D. I., Bourassa, M. A., Bradley, E. F., Clayson, C. A., de Leeuw, G., Drennan, W. M., Gille, S. T., Gulev, S. K., Kent, E. C., McGillis, W. R., Quartly, G. D., Ryabinin, V., Smith, S. R., Weller, R. A., Yelland, M. J., and Zhang, H.-M.: Observations to quantify air-sea fluxes and their role in climate variability and predictability, in: Proceedings of OceanObs'09: Sustained Ocean Observations and Information for Society, edited by: Hall, J., Harrison, D. E., and Stammer, D., European Space Agency, Noordwijk, The Netherlands, 299-313, 2010.

Frenger, I., Gruber, N., Knutti, R., and Münnich, M.: Imprint of Southern Ocean eddies on winds, clouds and rainfall, Nat. Geosci., 6, 608–612, doi:10.1038/ngeo1863, 2013.

Goswami, B. N.: A note on the deficiency of NCEP/NCAR reanalysis surface winds over the equatorial Indian Ocean, J. Geophys. Res., 108, 3124, doi:10.1029/2002jc001497, 2003.

Hogg, A. M. C., Dewar, W. K., Berloff, P., Kravtsov, S., and Hutchinson, D. K.: The effects of mesoscale ocean–atmosphere coupling on the large-scale ocean circulation, J. Climate, 22, 4066–4082, doi:10.1175/2009JCLI2629.1, 2009.

Josey, S. A.: A Comparison of ECMWF, NCEP–NCAR, and SOC Surface heat fluxes with moored buoy measurements in the subduction region of the Northeast Atlantic, J. Climate, 14, 1780–1789, doi:10.1175/1520-0442(2001)014<1780:acoenn>2.0.co;2, 2001.

Mauder, M., Liebethal, C., Göckede, M., Leps, J.-P., Beyrich, F., and Foken, T.: Processing and quality control of flux data during LITFASS-2003, Boundary-Layer Meteorology, 121, 67–88, doi:10.1007/s10546-006-9094-0, 2006.

Persson, P. O. G., Fairall, C. W., Andreas, E. L., Guest, P. S., and Perovich, D. K.: Measurements near the Atmospheric Surface Flux Group tower at SHEBA: near-surface conditions and surface energy budget, J. Geophys. Res., 107, 8045, doi:10.1029/2000JC000705, 2002.

Shi, R., Zeng, L., Chen, J., Yang, L., Dong, L., He, Y., Li, D., and Yao, J.: Observation and numerical simulation of the marine meteorology elements and air-sea fluxes at Yongxing Island in September 2013, Aquat. Ecosyst. Health, 18, 394–402, doi:10.1080/14634988.2015.1108822, 2015.

Smith, S. R., Legler, D. M., and Verzone, K. V.: Quantifying uncertainties in NCEP reanalyses using high-quality research vessel observations, J. Climate, 14, 4062–4072, doi:10.1175/1520-0442(2001)014<4062:quinru>2.0.co;2, 2001.

Sun, B., Yu, L., and Weller, R. A.: Comparisons of surface meteorology and turbulent heat fluxes over the Atlantic: NWP model analyses versus moored buoy observations, J. Climate, 16, 679–695, doi:10.1175/1520-0442(2003)016<0679:COSMAT>2.0.CO;2, 2003.

Swain, D., Rahman, S. H., and Ravichandran, M.: Comparison of NCEP turbulent heat fluxes with in situ observations over the south-eastern Arabian Sea, Meteorol. Atmos. Phys., 104, 163–175, doi:10.1007/s00703-009-0023-x, 2009.

Wang, D., Liu, Q., Huang, R. X., Du, Y., and Qu, T.: Interannual variability of the South China Sea throughflow inferred from wind data and an ocean data assimilation product, Geophys. Res. Lett., 33, L14605, doi:10.1029/2006gl026316, 2006.

Wang, D., Zeng, L., Li, X., and Shi, P.: Validation of satellite-derived daily latent heat flux over the South China Sea, compared with observations and five products, J. Atmos. Ocean. Tech., 30, 1820–1832, doi:10.1175/jtech-d-12-00153.1, 2013.

Wang, W. and McPhaden, M. J.: What is the mean seasonal cycle of surface heat flux in the equatorial Pacific? J. Geophys. Res., 106, 837–857, doi:10.1029/1999jc000076, 2001.

Wang, X., Zhang, R., Huang, J., Zeng, L., and Huang, F.: Biases of five latent heat flux products and their impacts on mixed-layer temperature estimates in the South China Sea, J. Geophys. Res., 122, 5088–5104, doi:10.1002/2016jc012332, 2017.

Weller, R. A. and Anderson, S. P.: Surface meteorology and air-sea fluxes in the Western equatorial Pacific warm pool during the TOGA Coupled Ocean-Atmosphere Response Experiment, J. Climate, 9, 1959–1990, doi:10.1175/1520-0442(1996)009<1959:smaasf>2.0.co;2, 1996.

Weller, R. A., Baumgartner, M. F., Josey, S. A., Fischer, A. S., and Kindle, J. C.: Atmospheric forcing in the Arabian Sea during 1994–1995: observations and comparisons with climatology and models, Deep Sea Research, Part II: Topical Studies in Oceanography, 45B, 1961–1999, doi:10.1016/s0967-0645(98)00060-5, 1998.

Yan, J.-Y., Tang, Z.-Y., Yao, H.-D., Li, J.-L., Xiao, Y.-G., and Chen, Y.-D.: Air-sea flux exchange over the Xisha Sea area before and after the onset of southwest monsoon in 2002, Chinese J. Geophys., 48, 1078–1090, doi:10.1002/cjg2.751, 2005.

Yan, J. Y., Yao, H. D., Li, J. L., Tang, Z. Y., Jiang, G. R., Sha, W. Y., Li, X. Q., and Xiao, Y. G.: Air-sea heat flux exchange over the South China Sea under different weather conditions before and after southwest monsoon onset in 2000, Acta Oceanol. Sin., 22, 369–383, 2003.

Yang, L., Wang, D., Huang, J., Wang, X., Zeng, L., Shi, R., He, Y., Xie, Q., Wang, S., Chen, R., Yuan, J., Wang, Q., Chen, J., Zu, T., Li, J., Sui, D., and Peng, S.: Toward a mesoscale hydrological and marine meteorological observation network in the South China Sea, B. Am. Meteorol. Soc., 96, 1117–1135, doi:10.1175/bams-d-14-00159.1, 2015.

Yu, L., Weller, R. A., and Sun, B.: Mean and variability of the WHOI daily latent and sensible heat fluxes at in situ flux measurement sites in the Atlantic Ocean, J. Climate, 17, 2096-2118, doi:10.1175/1520-0442(2004)017<2096:mavotw>2.0.co;2, 2004.

Yu, L., Jin, X., and Weller, R. A.: Multidecade global flux datasets from the objectively analyzed air-sea fluxes (OAFlux) project: latent and sensible heat fluxes, ocean evaporation, and related surface meteorological variables. http://oaflux.whoi.edu/pdfs/OAFlux_TechReport_3rd_release.pdf, last access: 19 September 2017, 2008.

Yu, L., Jin, X., and Weller, R. A.: Role of net surface heat flux in seasonal variations of sea surface temperature in the tropical Atlantic Ocean, J. Climate, 19, 6153–6169, doi:10.1175/jcli3970.1, 2006.

Zeng, L., Shi, P., Liu, W. T., and Wang, D.: Evaluation of a satellite-derived latent heat flux product in the South China Sea: a comparison with moored buoy data and various products, Atmos. Res., 94, 91–105, doi:10.1016/j.atmosres.2008.12.007, 2009.

Zeng, X., Zhao, M., and Dickinson, R. E.: Intercomparison of bulk aerodynamic algorithms for the computation of sea surface fluxes using TOGA COARE and TAO data, J. Climate, 11, 2628–2644, doi:10.1175/1520-0442(1998)011<2628:iobaaf>2.0.co;2, 1998.

Zhang, R., J. Huang, X. Wang, J. A. Zhang, and F. Huang, 2016: Effects of Precipitation on Sonic Anemometer Measurements of Turbulent Fluxes in the Atmospheric Surface Layer. J. Ocean Univ. China, 15(3), 389–398. doi:10.1007/s11802-016-2804-4.

Zhu, J., Kamachi, M., and Wang, D.: Estimation of air-sea heat flux from ocean measurements: an ill-posed problem, J. Geophys. Res., 107, 3159, doi:10.1029/2001jc000995, 2002.

带格式的：字体：（默认）Times New Roman，（中文）Times New Roman，字体颜色：自动设置，图案：清除

Figure captions

Figure 1. (a) Yongxing Island air-sea flux tower (YXASFT).

(b) Instrumentation and data acquisition system mounted on the YXASFT.

(c) Pictures of some sensors on the YXASFT.

(d) Google satellite image of Yongxing Island. The red triangle indicates the location of the YXASFT.

(e) Map of the northern SCS. The black star indicates the location of Yongxing Island.

~~Figure 1. (a) Yongxing Island air-sea flux tower (YXASFT).~~

~~(b) Google satellite image of Yongxing Island. The red triangle indicates the location of the YXASFT.~~

~~(c) Instrumentation and data acquisition system mounted on the YXASFT.~~

~~(d) Map of the northern SCS. The black star indicates the location of Yongxing Island.~~

~~(e) Pictures of some sensors on the YXASFT.~~

Figure 2. Diagram of the real-time data acquisition system and the sensor wiring scheme on the YXASFT (SEx: single-ended channel; VXx: voltage excitation channel; Px: pulse-input channel; IXx: current excitation channel; SDM: SDM channel; (Campbell Scientific, Inc. 2018) GPRS: General Packet Radio Service; CDMA: code-division multiple access).

Figure 3 EC turbulence data processing and quality control flow chart

Figure 43. Daily means of the LHF and SHF time series (top panels) and scatter plots (bottom panels) of COARE3.0 versus ECF (from 2016/02/01 to 2016/03/29). The R^2 values, linear regressions and numbers of matched pairs (N) are given in the bottom panels. The solid red line refers to the linear regression of the matched pairs. The solid green line y=x indicates a 1:1 correspondence.

Figure 45. Daily mean time series plots of the YXASFT-observed (red solid lines) and OAFlux-analyzed (blue solid lines) U, Qa, Ta, and Ts values over the study period (2016/02/01-2017/01/31).

Figure 56. Daily mean time series plots of the YXASFT-observed (red solid lines) and OAFlux-analyzed (blue solid lines) SHF and LHF over the study period (2016/02/01-2017/01/31).

Figure 67. Scatter plots of the YXASFT and OAFlux wind speeds at 10 m (U), air specific humidities at 2 m (Qa), and sea surface temperatures (Ts) and air temperatures at 2 m (Ta) during the spring (left column), summer _autumn (middle column), and winter (right column) periods. The units for U, Qa, Ts and Ta are m/s, g/kg, ℃ and ℃, respectively. The linear regression equation, coefficient of determination (R^2), and number of matched pairs (N) are given in each panel. The solid red line refers to the linear regression of the matched pairs.

Figure 78. Daily mean time series plots of the YXASFT-observed downward long radiation (DLR) over the study period (2016/02/01-2017/01/31).

Figure 89. Same as Fig. 5 but for LHF (first row) and SHF (second row).

Figure 910. Scatter plots for the biases of U (ΔU), Qa (ΔQa), Ts (ΔTs), and Ta (ΔTa) with respect to the biases of LHF (ΔLHF). All of the data are normalized to the range of -10 to 10 in this paper. The linear regression equation and coefficient of determination (R^2) are given in each panel. The solid red line refers to the linear regression of the matched pairs.

Figure 1011. Same as Fig. 9 but for the biases in SHF.

带格式的：字体：（中文）Times New Roman

带格式的：字体：（中文）Times New Roman

带格式的：字体：小五

带格式的：字体：（中文）+中文正文（宋体），（中文）中文(中国)

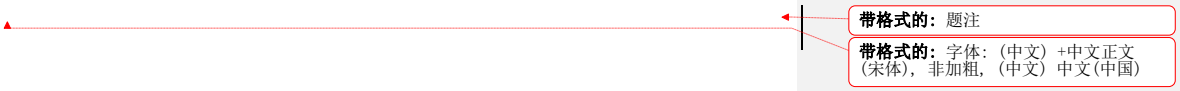
带格式的：题注
带格式的：字体：（中文）+中文正文（宋体），非加粗，（中文）中文(中国)

Tables

Table 1. List of sensors installed on the YXASFT and their specifications

Parameters	Sensor	Scan interval (Hz)	Averaging interval (min)	Installation height (m)
Wind speed and direction	Young 05106	1	1, 10, 30	5, 10, 15, 20
Air temperature and humidity	Vaisala HMP155A	1	1, 10, 30	5, 10, 15, 20
Four-component radiation	Hukseflux NR01	1	1, 10, 30	8
Sea surface temperature	Campbell SI-112	1	1, 10, 30	5
Eddy turbulent fluxes (u, v, w, t, ρ_v, T_{au}, SHF, LHF, F_c)	Campbell IRGASON	10	30	12

Table 2. Information regarding the adopted in situ and reanalysis data*

Data	Variables	Location	Height (m)	Interval	Period (day)
In situ bulk variables	U	112.33° E, 16.84° N	10	30 min	366
	Q_a		5	30 min	
	T_s		0.05	30 min	
	T_a		5	30 min	
	DLR		8	30 min	
In situ bulk heat fluxes	SHF		10	30 min	
	LHF		10	30 min	
In situ ECF turbulent data	u		12	0.1 sec	57
	v		12	0.1 sec	
	w		12	0.1 sec	
	t		12	0.1 sec	
	ρ_v		12	0.1 sec	
	SHF		12	30 min	
	LHF		12	30 min	
OAFlux bulk variables And heat fluxes	U	111.5° E, 16.5° N	10	1 day	366
	Q_a		2		
	T_s	112.5° E, 16.5° N	0.05		
	T_a	112.5° E, 15.5° N	2		
	SHF	111.5° E, 15.5° N	10		
	LHF		10		

u: wind speed along the sonic x-axis, v: wind speed along the sonic y-axis, w: wind speed along the sonic z-axis, t: sonic temperature, ρ_v: water vapor density. The height of the bulk fluxes derived via COARE3.0 for both in situ data and OAFlux are considered at 10 m.

Table 3. Quantitative statistical summary based on comparisons between daily YXASFT measurements and daily OAFlux products in the spring, summer_ autumn, and winter Periods

Season	Variable	OAFlux mean	YXASFT mean	*RMSE*	*Bias*	R^2	Regression	
							C_1	C_2
Spring	*U* (m/s)	7.36	6.40	1.36	0.96	0.90	0.89	1.66
	Q_a (g/kg)	15.29	15.63	1.27	-0.33	0.81	0.57	6.42
	T_a (℃)	24.10	24.62	0.68	0.52	0.92	0.90	2.06
	T_s (℃)	25.12	24.65	1.29	0.46	0.47	0.32	17.27
	SHF (w/m^2)	15.46	-1.37	25.64	16.83	0.01	-0.45	14.84
	LHF (w/m^2)	123.87	72.92	63.23	50.95	0.80	1.42	20.39
Summer_Autumn	*U* (m/s)	6.16	4.97	1.67	1.19	0.79	0.85	1.93
	Q_a (g/kg)	20.33	21.08	1.09	-0.75	0.68	0.66	6.47
	T_a (℃)	28.86	28.95	0.43	-0.10	0.84	1.00	-0.09
	T_s (℃)	29.04	29.11	0.61	-0.07	0.70	0.70	8.62
	SHF (w/m^2)	1.65	0.51	6.33	1.07	0.31	1.10	1.02
	LHF (w/m^2)	97.97	55.98	50.49	42.43	0.40	0.94	46.04
Winter	*U* (m/s)	10.07	9.40	0.93	0.67	0.92	0.95	1.14
	Q_a (g/kg)	16.35	16.47	0.67	-0.11	0.80	0.71	4.60
	T_a (℃)	24.91	25.48	0.67	-0.57	0.89	0.90	1.95
	T_s (℃)	25.72	25.67	0.68	0.05	0.54	0.50	12.90
	SHF (w/m^2)	13.83	9.73	28.85	23.56	0.14	-1.59	-1.62
	LHF (w/m^2)	148.32	85.03	72.35	63.29	0.66	1.30	37.45

*OAFlux = $C_1 \times$ YXASFT+C_2

Figures

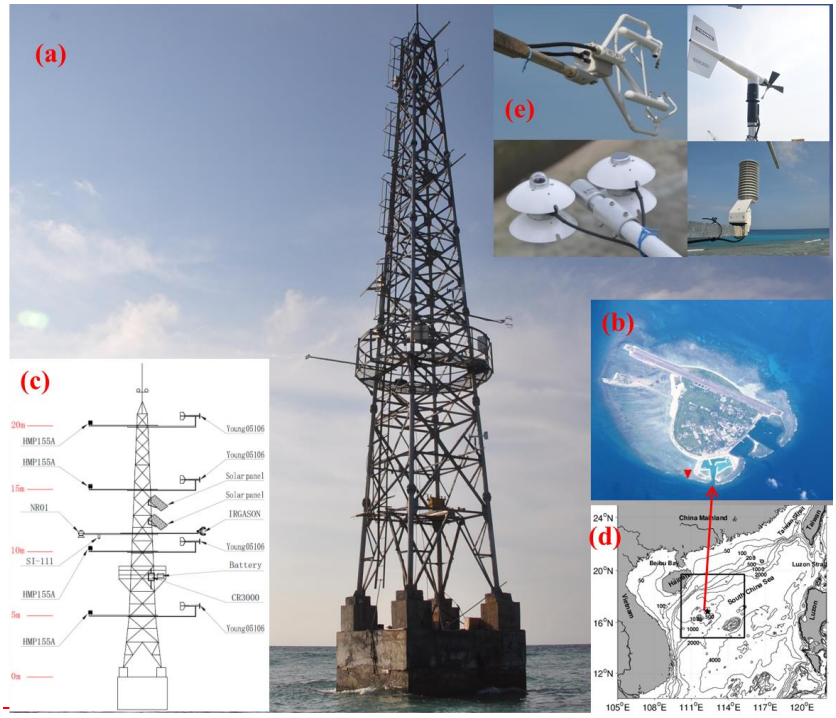
(a)
(e)
(b)
(c)
(d)
20m
HMP155A
Young05106
15m
NR01
IRGASON
10m
SI-111
Battery
CR3000
5m
0m
China Mainland
Bohai Sea
South China Sea
Vietnam
Luzon
Luzon Strait
24°N
20°N
16°N
12°N
105°E
108°E
111°E
114°E
117°E
120°E

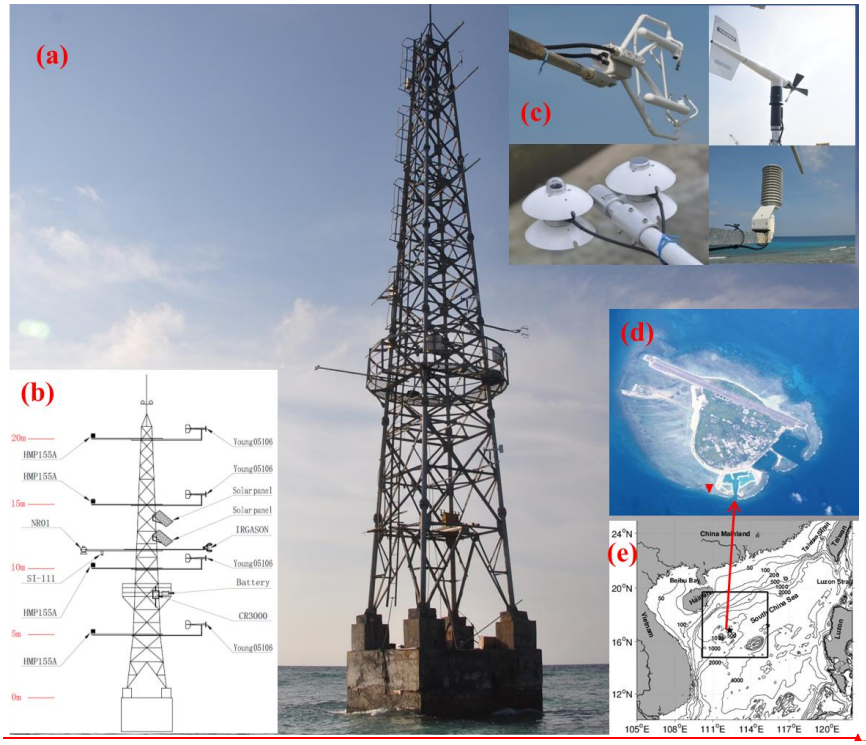

Figure 1

带格式的：字体：（中文）+中文正文（宋体），（中文）中文(中国)

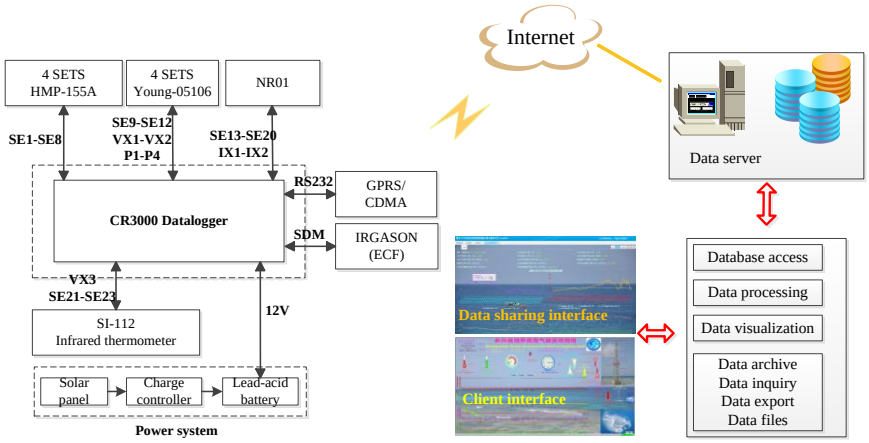
Internet
4 SETS
HMP-155A
4 SETS
Young-05106
NR01
SE1-SE8
SE9-SE12
VX1-VX2
P1-P4
SE13-SE20
IX1-IX2
CR3000 Datalogger
RS232
GPRS/
CDMA
SDM
IRGASON
(ECF)
VX3
SE21-SE23
12V
SI-112
Infrared thermometer
Solar
panel
Charge
controller
Lead-acid
battery
Power system
Data server
Data sharing interface
Client interface
Database access
Data processing
Data visualization
Data archive
Data inquiry
Data export
Data files

Figure 2

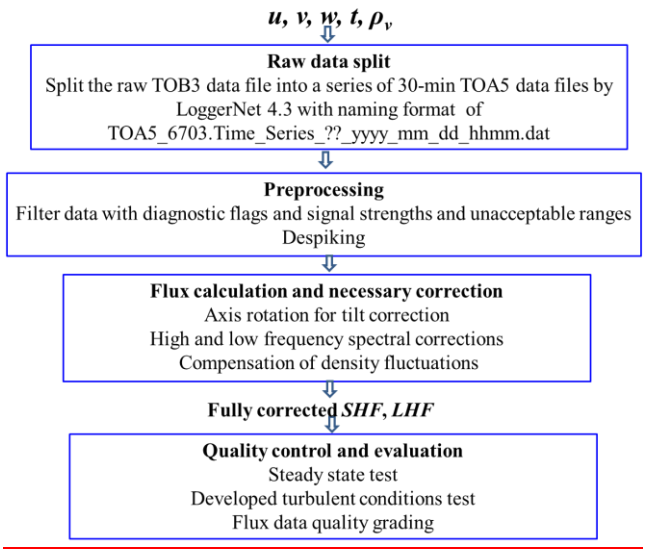

Figure 3

带格式的：字体：（中文）+中文正文（宋体），（中文）中文(中国)

带格式的：字体：（中文）+中文正文（宋体），（中文）中文(中国)

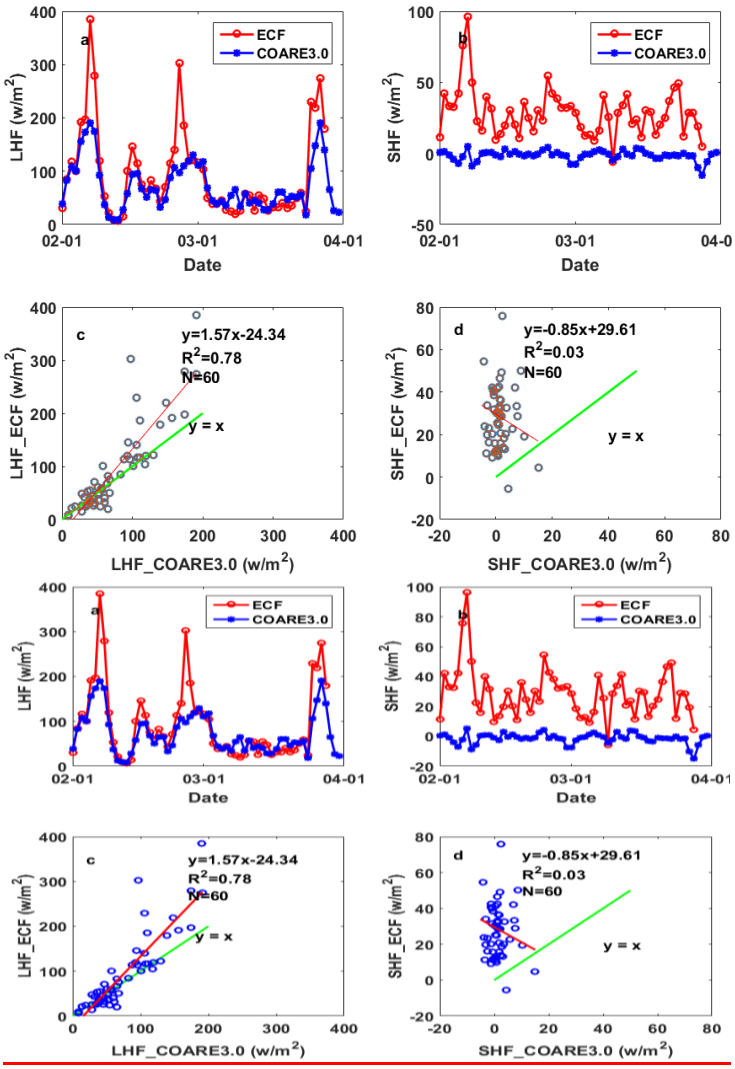

Figure 43

带格式的：左

带格式的：字体：（中文）+中文正文（宋体），（中文）中文(中国)

带格式的：列出段落，缩进：左侧：2.12 厘米，右 4.24 字符

带格式的：字体：（中文）+中文正文（宋体），（中文）中文(中国)

带格式的：题注

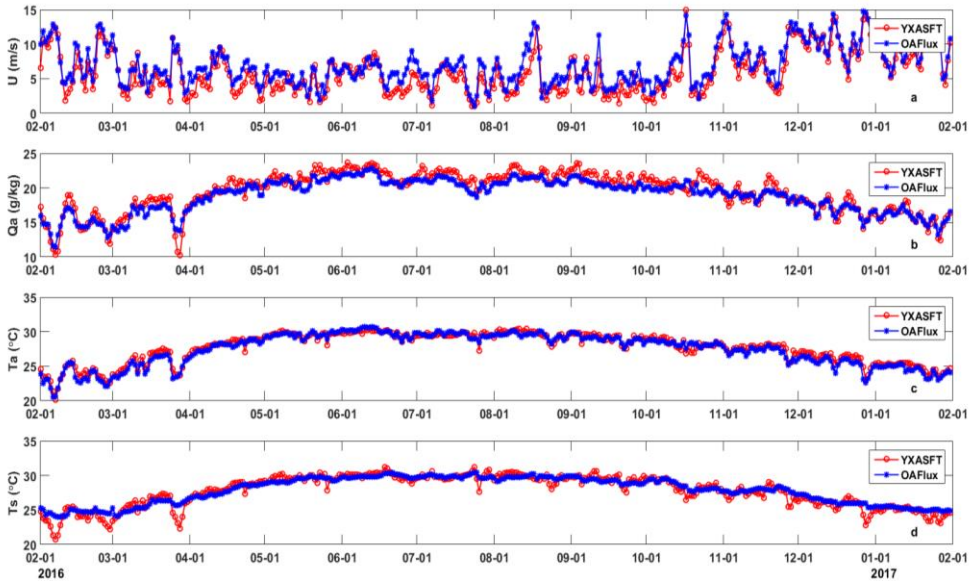

Figure 54

带格式的：字体：（中文）+中文正文（宋体），（中文）中文(中国)

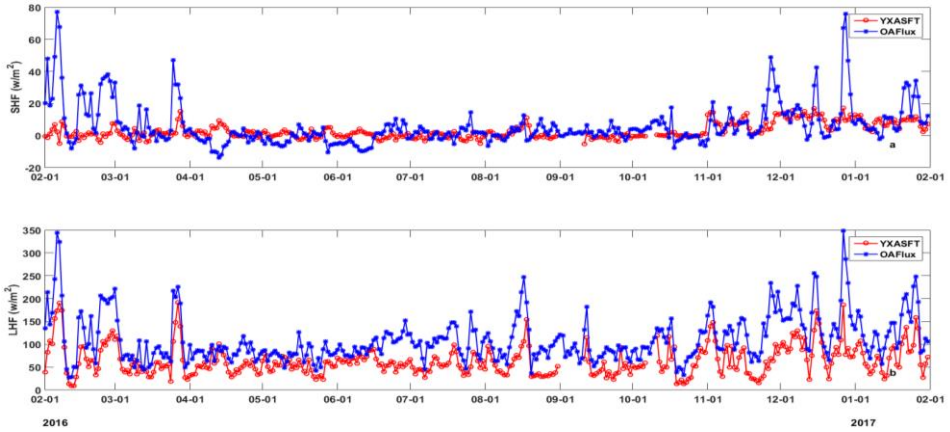

Figure ~~5~~6

带格式的：字体：（中文）+中文正文（宋体），（中文）中文(中国)

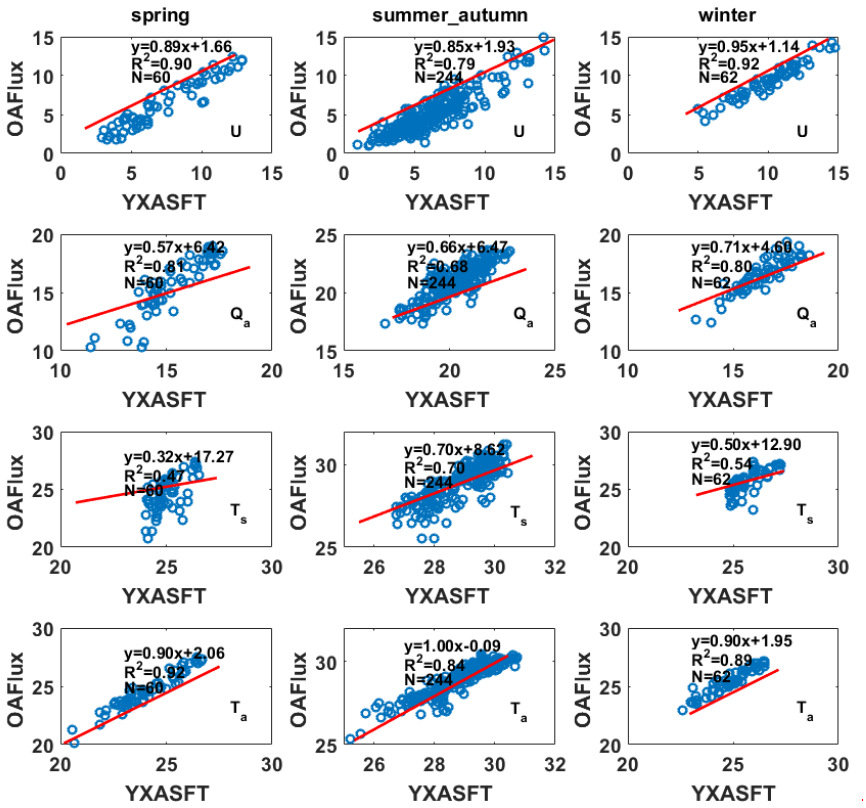
spring
summer_autumn
winter
y=0.89x+1.66
R2=0.90
N=60
y=0.85x+1.93
R2=0.79
N=244
y=0.95x+1.14
R2=0.92
N=62
U
y=0.57x+6.42
R2=0.81
N=60
y=0.66x+6.47
R2=0.68
N=244
y=0.71x+4.68
R2=0.80
N=62
Qa
y=0.32x+17.27
R2=0.47
N=60
y=0.70x+8.62
R2=0.70
N=244
y=0.50x+12.90
R2=0.54
N=62
Ts
y=0.90x+2.06
R2=0.92
N=60
y=1.00x-0.09
R2=0.84
N=244
y=0.90x+1.95
R2=0.89
N=62
Ta
OAFlux
YXASFT

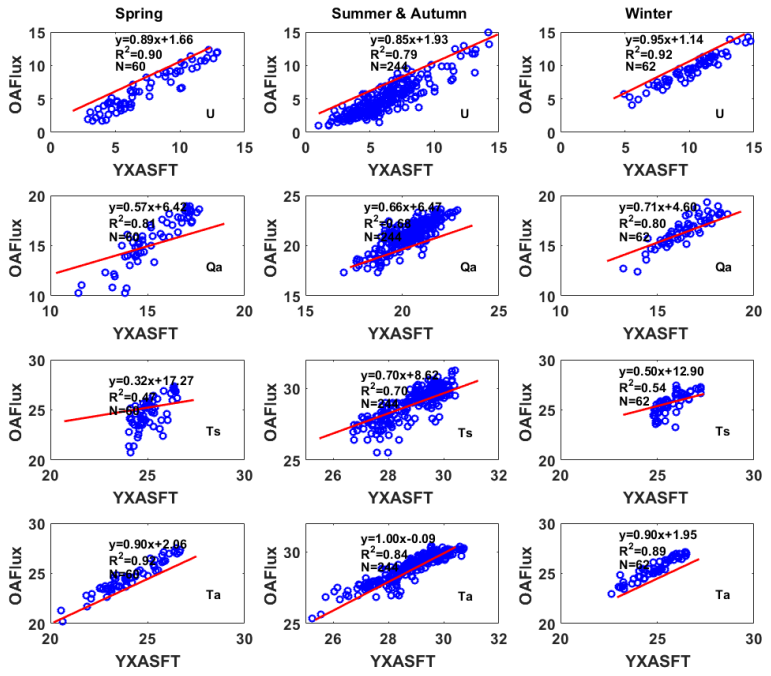
Spring
Summer & Autumn
Winter
y=0.89x+1.66
R2=0.90
N=60
y=0.85x+1.93
R2=0.79
N=244
y=0.95x+1.14
R2=0.92
N=62
U
y=0.57x+6.47
R2=0.81
N=60
y=0.66x+6.47
R2=0.68
N=244
y=0.71x+4.60
R2=0.80
N=62
Qa
y=0.32x+17.27
R2=0.47
N=60
y=0.70x+8.62
R2=0.70
N=244
y=0.50x+12.90
R2=0.54
N=62
Ts
y=0.90x+2.06
R2=0.93
N=60
y=1.00x-0.09
R2=0.84
N=244
y=0.90x+1.95
R2=0.89
N=62
Ta
OAFlux
YXASFT

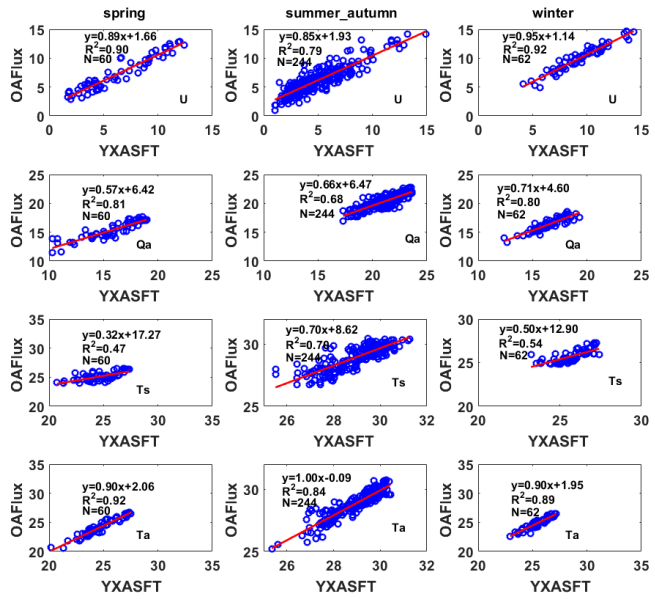

Figure ~~67~~

带格式的： 字体：（中文）+中文正文（宋体），（中文）中文(中国)

带格式的： 字体：（中文）+中文正文（宋体），（中文）中文(中国)

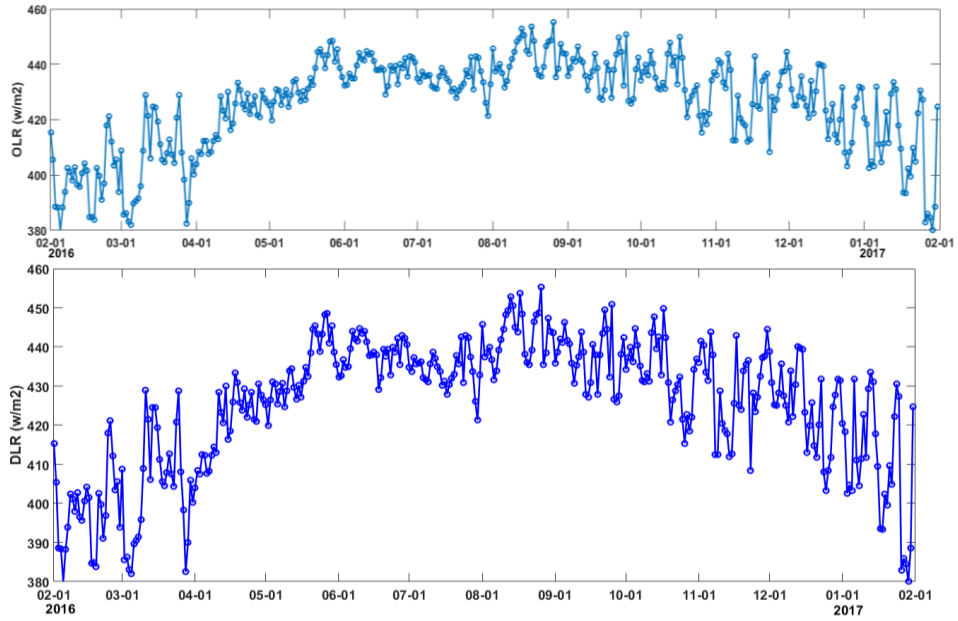

Figure ~~7~~8

带格式的： 字体：（中文）+中文正文（宋体），（中文）中文(中国)

带格式的： 字体：（中文）+中文正文（宋体），（中文）中文(中国)

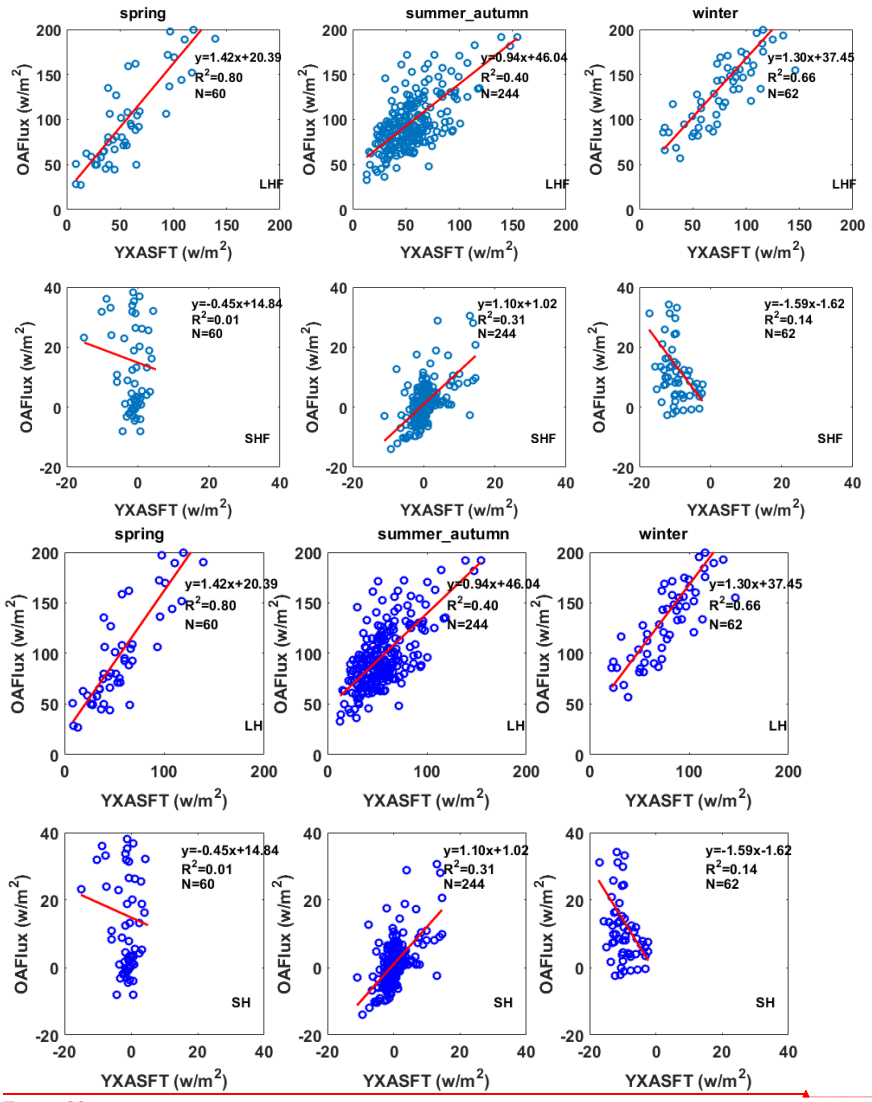

Figure ~~89~~

带格式的：字体：（中文）+中文正文（宋体），（中文）中文(中国)

带格式的：正文

带格式的：字体：（中文）+中文正文（宋体），（中文）中文(中国)

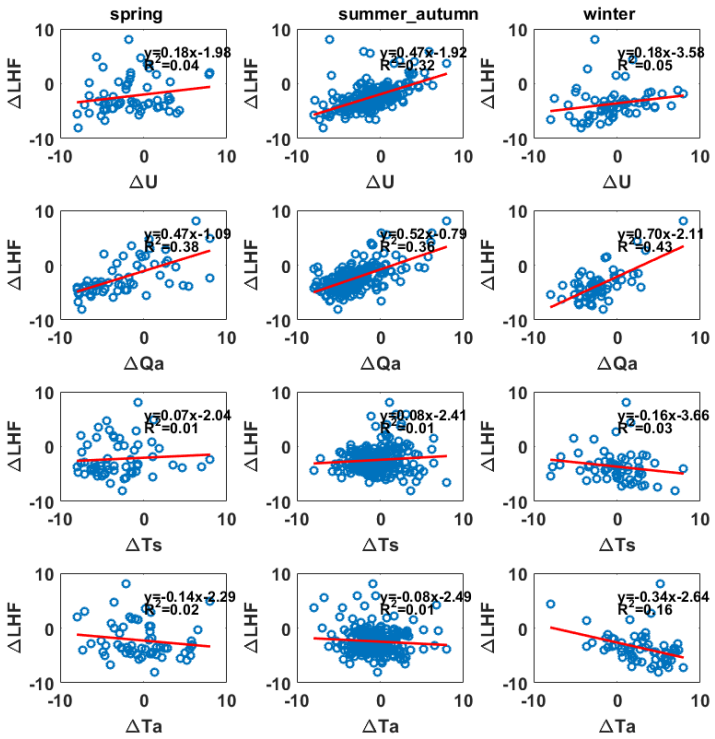
spring
summer_autumn
winter
y=0.18x-1.98
R²=0.04
y=0.47x-1.92
R²=0.32
y=0.18x-3.58
R²=0.05
y=0.47x-1.09
R²=0.38
y=0.52x-0.79
R²=0.38
y=0.70x-2.11
R²=0.43
y=0.07x-2.04
R²=0.01
y=0.08x-2.41
R²=0.01
y=-0.16x-3.66
R²=0.03
y=-0.14x-2.29
R²=0.02
y=-0.08x-2.49
R²=0.01
y=-0.34x-2.64
R²=0.16
ΔLHF
ΔU
ΔQa
ΔTs
ΔTa

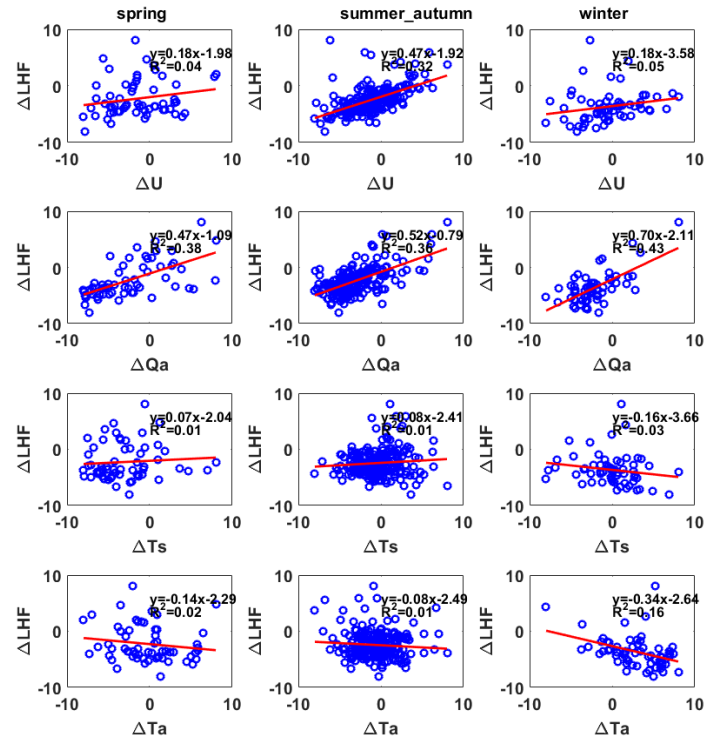

Figure 910

带格式的：字体：（中文）+中文正文（宋体），（中文）中文(中国)

带格式的：字体：（中文）+中文正文（宋体），（中文）中文(中国)

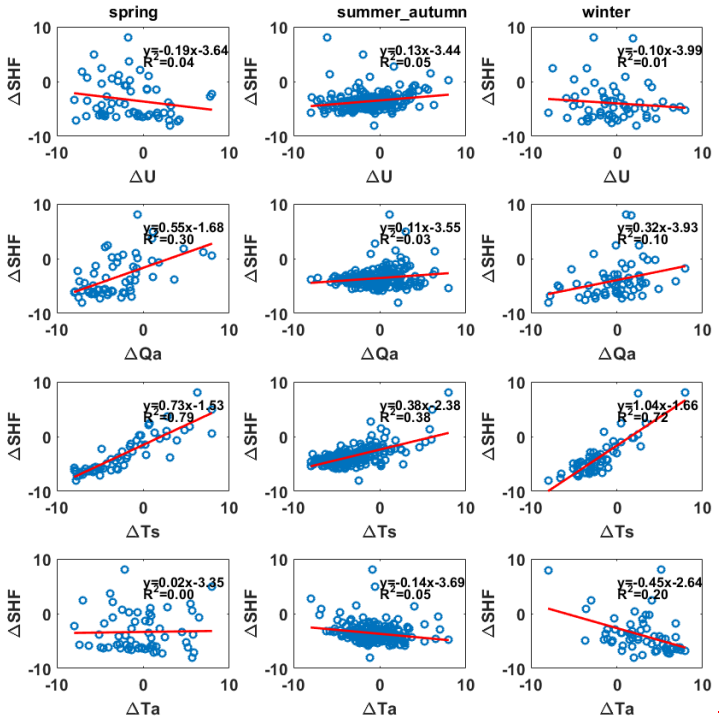
spring
summer_autumn
winter
y=-0.19x-3.64
R²=0.04
y=0.13x-3.44
R²=0.05
y=-0.10x-3.99
R²=0.01
y=0.55x-1.68
R²=0.30
y=0.11x-3.55
R²=0.03
y=0.32x-3.93
R²=0.10
y=0.73x-1.53
R²=0.79
y=0.38x-2.38
R²=0.38
y=1.04x-1.66
R²=0.72
y=0.02x-3.35
R²=0.00
y=-0.14x-3.69
R²=0.05
y=-0.45x-2.64
R²=0.20
ΔSHF
ΔU
ΔQa
ΔTs
ΔTa

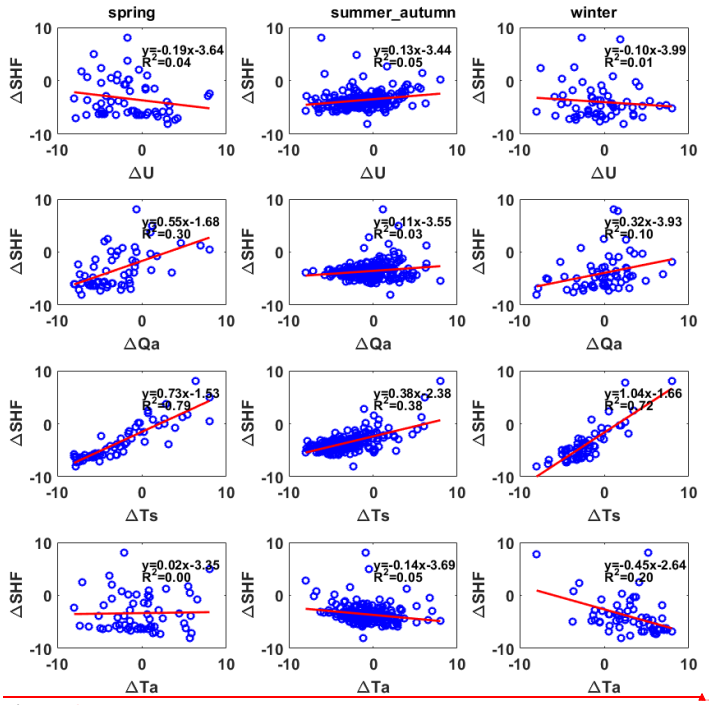

Figure ~~10~~11

带格式的：字体：（中文）+中文正文（宋体），（中文）中文(中国)

带格式的：字体：（中文）+中文正文（宋体），（中文）中文(中国)